

Searching for Associations Between Short Gamma-ray Bursts and Fast Radio Bursts

MING-XUAN LU,¹ LONG LI,² XIANG-GAO WANG,¹ CAN-MIN DENG,¹ YUN-FENG LIANG,¹ DA-BIN LIN,¹ AND EN-WEI LIANG¹

¹*Guangxi Key Laboratory for Relativistic Astrophysics, School of Physical Science and Technology, Guangxi University, Nanning 530004, China*

²*Department of Astronomy, School of Physical Sciences, University of Science and Technology of China, Hefei 230026, China*

ABSTRACT

The physical origin of fast radio bursts (FRBs) is still unclear. However, young magnetars associated with short-duration gamma-ray bursts (SGRBs) have been thought to be possible central engines for some FRBs. In this paper, we perform a systematic search for SGRBs that are associated with FRBs in a sample including 623 FRBs (601 one-off bursts and 22 repeaters) and 168 SGRBs with precise localizations. We find that FRB 190309A is spatially associated with GRB 060502B, with a chance probability of 0.05 when temporal and redshift information is taken into account. Considering the high chance probability (the statistical significance is $< 3\sigma$), we examine other observational properties such as the host galaxy, the dispersion measure, and the energy budget of the central engine to check the possibility of their association. Although the available observational information is insufficient to determine whether they are physically associated, it does not rule out such a possibility. As the only pair of FRB and GRB that are spatially associated, it remains an interesting case worthy of further attention.

Keywords: Radio transient sources (2008) — Gamma-ray bursts (629) — Magnetars (992)

1. INTRODUCTION

Fast radio bursts (FRBs) are mysterious radio transients with millisecond durations (Lorimer et al. 2007; Thornton et al. 2013; Platts et al. 2019). FRBs have extremely high brightness temperatures (Cordes & Chatterjee 2019; Petroff et al. 2019). The dispersion measures (DMs) of FRBs exceed the Milky Way’s contribution and some of them have been reliably determined to be located in the extragalactic systems (Chatterjee et al. 2017; Bannister et al. 2019; Prochaska et al. 2019; Ravi et al. 2019; Marcote et al. 2020). Up to now, except for the X-ray burst from the Galactic soft gamma repeater (SGR) SGR1935+2154 coincident with the fast radio burst FRB200428 (Bochenek et al. 2020; CHIME/FRB Collaboration et al. 2020), no other multiwavelength/multimessenger transients associated with FRBs are definitely observed (Yamasaki et al. 2016; DeLaunay et al. 2016; Hardy et al. 2017; Zhang & Zhang 2017; Xi et al. 2017; James et al. 2019; Cunningham et al. 2019; Mereghetti et al. 2020; Tavani et al. 2020; Xin et al. 2021; Li et al. 2021; The LIGO Scientific Collaboration et al. 2022; Wang & Nitz 2022), though there have been some works claiming tentative associations of FRBs with multiwavelength transient counterparts (Wang et al. 2020b; Li et al. 2022). Current FRB models can be divided into two categories: catastrophic models (e.g., Kashiyama et al. 2013; Totani 2013; Falcke & Rezzolla 2014; Zhang 2014, 2016; Liu et al. 2016; Wang et al. 2016) and non-catastrophic models (e.g., Dai et al. 2016; Murase et al. 2016; Metzger et al. 2017; Margalit & Metzger 2018; Zhang 2020; Ioka & Zhang 2020; Wang et al. 2020a; Geng et al. 2021; Deng et al. 2021). The former (e.g. NS-NS merger or NS-BH merger model with NS and BH denoting neutron star and black hole, respectively) is invoked to explain one-off FRBs. The latter usually invokes a NS born in a catastrophic event as the central engine of the FRB.

The localization of FRB sources and the identification of their host galaxies are important for understanding their physical origins, and several host galaxies of FRBs have been identified. The host galaxy of the first repeat source

Corresponding author: Xiang-Gao Wang

E-mail: wangxg@gxu.edu.cn

FRB 121102 is found to be similar to the host galaxies of superluminous supernovae (SLSNe) and long gamma-ray bursts (LGRBs) (Tendulkar et al. 2017; Nicholl et al. 2017; Metzger et al. 2017; Tendulkar et al. 2017; Chatterjee et al. 2017; Marcote et al. 2017; Zhang & Wang 2019). However, the host environment of another well-localized repeater FRB 20180916B is completely different to FRB 121102 (Tendulkar et al. 2021). The one-off bursts FRB 190523A and FRB 180924B are found to occur in massive galaxies with low star formation rates and have large offsets from the centers of their hosts (Ravi et al. 2019; Bannister et al. 2019). These two FRBs share similar properties with the host environments of short gamma-ray bursts (SGRBs) and binary neutron star (BNS) mergers (Margalit et al. 2019; Gourdji et al. 2020). In addition, Li et al. (2019) also suggested that some FRB host candidates have low star formation and large offsets, and the corresponding FRBs may be driven by NSs that were born in BNS mergers.

Gamma-ray bursts (GRBs) are the most luminous explosions in the universe. Based on the duration distribution, they can be divided into LGRBs and SGRBs with a separation line of about 2 seconds (Kouveliotou et al. 1993; Kumar & Zhang 2015; Zhang 2018b). For SGRBs, the NS-NS or NS-BH merger is the preferred progenitor model. The joint detection of an SGRB and the gravitational wave event confirms the NS-NS merger origin for at least some SGRBs (Abbott et al. 2017b; Goldstein et al. 2017). Although the event rate of SGRBs is much smaller than that of FRBs, we believe that some FRBs may be related to SGRBs for the following reasons: 1. Several theoretical models predict FRB emissions are also in connection with neutron star mergers (Totani 2013; Wang et al. 2016; Zhang 2020). 2. The BNS merger may leave behind a massive, stable, rapidly-spinning magnetar that could serve as the central engine of SGRB, which could also power FRBs after an uncertain time delay (Popov & Postnov 2013; Lyubarsky 2014; Kulkarni et al. 2014; Gao et al. 2016; Katz 2016; Yang & Zhang 2018; Lu & Kumar 2018; Margalit et al. 2019; Wang et al. 2020a; Lin & Totani 2020; Beloborodov 2020). 3. For most host galaxies of one-off FRBs, their properties are similar to the host galaxies of SGRBs, which have low star formation rates and large offsets from the centers of the galaxies (Barthelmy et al. 2005; Gehrels et al. 2005; Fox et al. 2005; Bloom et al. 2006b; Fong et al. 2013; Bannister et al. 2019; Ravi et al. 2019; Marcote et al. 2020; Wang et al. 2020a).

Searches for continuous radio emission and/or FRBs associated with SGRBs have been conducted in many works but have not revealed a reliable association (Dessenne et al. 1996; Bannister et al. 2012; Obenberger et al. 2014; Palaniswamy et al. 2014; Kaplan et al. 2015; Anderson et al. 2018; Rowlinson et al. 2019; Anderson et al. 2021; Rowlinson et al. 2021; Tian et al. 2022). It is valuable to study the connection between SGRBs and FRBs with large FRB and SGRB samples (Curtin et al. 2022). Recently, the Canadian Hydrogen Intensity Mapping Experiment (CHIME) released a large sample of FRBs (The CHIME/FRB Collaboration et al. 2021). In this work, we perform a systematic search for SGRBs that may be associated with FRBs in the SGRB and FRB samples which include all publicly reported FRBs and precisely-localized SGRBs before September 2022, making our work the one considering the most complete samples to date.

2. SEARCH FOR FRBS ASSOCIATED WITH SGRBS

The first FRB was reported in 2007 (Lorimer et al. 2007). Since then, 807 FRBs have been reported in the literature until September 2022, including 601 one-off bursts and 204 repeat bursts from 22 repeaters¹ (Petroff & Yaron 2020). For the SGRB sample, we consider the GRB catalog² presented by J. Greiner (JG catalog), which compiles GRBs detected by various detectors, e.g., Fermi, Swift, HETE-2, BeppoSAX, BATSE, AGILE, etc. The JG catalog contains thousands of objects and is updated almost every day. Until September 2022, there are more than one thousand GRBs with afterglow detections recorded in the JG catalog. In general, T_{90} is used to categorize LGRBs ($T_{90} > 2$ s) and SGRBs ($T_{90} \leq 2$ s), and there are 111 SGRBs with afterglow detections in the JG catalog (we have also checked the *Swift*/XRT website³ and confirmed that there are no other SGRBs with afterglow detections by *Swift*/XRT). In addition, some GRBs with the T_{90} larger than 2s are also classified as SGRBs because there is evidence that they are of merger origin, which include 19 SGRBs ($T_{90} > 2$ s). In total, there are 130 SGRBs with afterglow detections in our sample. In addition, considering the excellent localization capability of *Swift*/BAT, we also use the SGRBs detected by *Swift*/BAT even without an afterglow detection (38 SGRBs). We list our SGRB sample in Table 1. Figure 1 shows the sky distribution of our sample, including 168 SGRBs and 623 FRBs (601 one-off bursts and 22 repeaters).

We perform a systematic search of our sample based on the following three criteria (Wang et al. 2020b): I, the SGRB should positionally overlap with the FRB within the localization error circle; II, the SGRB should occur earlier

¹ <https://www.wis-tns.org>

² <https://www.mpe.mpg.de/~jcg/grbgen.html#userconsent#>

³ https://swift.gsfc.nasa.gov/archive/grb_table.html/

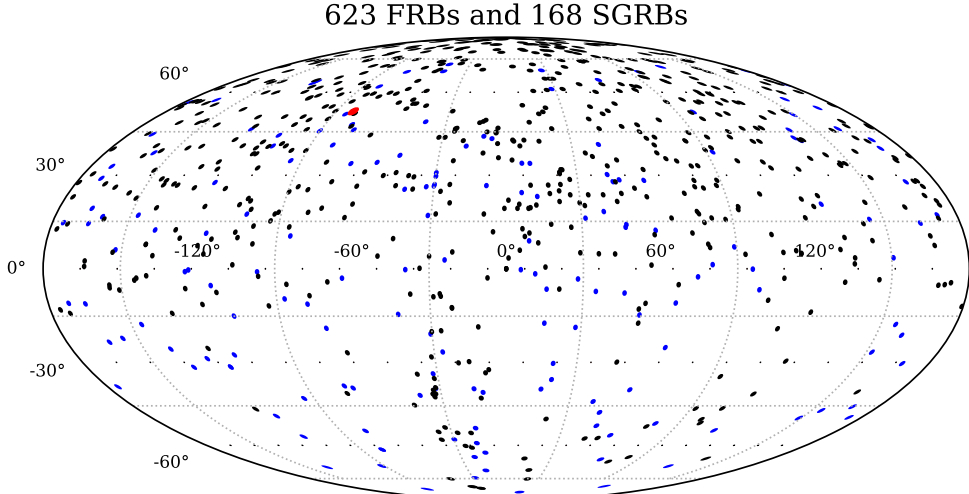


Figure 1. Sky distributions in celestial coordinates of the 623 FRBs and 168 SGRBs considered in this work. The black points represent the positions of the FRBs. The blue points represent the locations of SGRBs. The region enclosing GRB 060502B and FRB 190309A is marked by a red circle.

than the FRB; III, the redshift of the SGRB should be compatible with the FRB distance derived from its DM. The criterion III is described in more detail below.

The observed total DMs can usually be composed of

$$\text{DM}_{\text{total,obs}} = \text{DM}_{\text{MW}} + \text{DM}_{\text{IGM}} + \frac{\text{DM}_{\text{host}}}{1+z} \quad (1)$$

where DM_{MW} is the DM contribution from the Milky Way, the DM_{IGM} is the DM contribution from intergalactic medium (IGM) and DM_{host} is the DM contribution from the FRB host galaxy. Although for a single FRB the relationship between DM_{IGM} and redshift is difficult to be determined, a mean value can be estimated through (Zhang 2018a; Deng et al. 2019)

$$\overline{\text{DM}}_{\text{IGM}}(z) = \frac{3cH_0\Omega_b f_{\text{IGM}}f_e}{8\pi Gm_p} \int_0^z \frac{1+z'}{E(z')} dz' \quad (2)$$

where $E(z') = H(z')/H_0$ with H_0 the Hubble constant, Ω_b is the baryon density, $f_{\text{IGM}} \sim 0.83$ is the fraction of baryons in IGM (Fukugita et al. 1998), m_p is the proton mass, and the number of free electrons per baryon in the universe is $f_e \sim 7/8$ (Deng & Zhang 2014). The Λ CDM cosmological parameters of the Planck results are adopted, i.e., $H_0=67.74$ km s⁻¹ Mpc⁻¹, $\Omega_m = 0.3089$, $\Omega_\Lambda = 0.6911$, and $\Omega_b = 0.0486$ (Planck Collaboration et al. 2016). Because Eq. (2) assumes that the matter in the IGM is uniformly distributed, the effects of inhomogeneities should also be considered, leading to an uncertainty $\sigma_{\text{IGM}}(z)$ of the $\overline{\text{DM}}_{\text{IGM}}(z)$ (McQuinn 2014). Thus, we have to take into account the $\sigma_{\text{IGM}}(z)$ when converting a redshift into DM_{IGM} . This means that for a given redshift, a DM range of $\overline{\text{DM}}_{\text{IGM}}(z) \pm \sigma_{\text{IGM}}(z)$ is acceptable. The criterion III requires this range covers the $\text{DM}_{\text{IGM}} = \text{DM}_{\text{total,obs}} - \text{DM}_{\text{MW}} - \text{DM}_{\text{host}}/(1+z)$. We use the results in McQuinn (2014) to obtain the value of σ_{IGM} and adopt the baryon distribution model that considers the details of the accretion rates of baryons into dark matter halos.

The DM_{MW} values have been provided in the FRB catalog (Petroff & Yaron 2020), which are derived based on two Galactic electron models (Cordes & Lazio 2002; Yao et al. 2017). However, only a handful of FRBs have the measurements of DM_{host} to date (e.g., FRB 121102 (Tendulkar et al. 2017), FRB 171020 (Mahony et al. 2018), FRB 200120E (Bhardwaj et al. 2021a)). Therefore, we adopt the $\text{DM}_{\text{obs}} - \text{DM}_{\text{MW}}$ as a proxy / an upper limit of the DM_{IGM} (i.e., ignoring the DM contribution from the host galaxy). We have tested that assuming a typical value of 50 of the DM_{host} (Deng et al. 2019) would not change our main conclusions. By requiring $\overline{\text{DM}}_{\text{IGM}}(z)$

$\pm \sigma_{\text{IGM}}(z)$ covers the $\text{DM}_{\text{IGM}} = \text{DM}_{\text{obs}} - \text{DM}_{\text{MW}}$, we estimate the redshift range compatible with the observed DM for each FRB in our sample. Only one pair of SGRB and FRB satisfies the three criteria (in fact, only this pair satisfies criterion I): GRB 060502B and FRB 190309A. The position of GRB 060502B located by *Swift*/XRT is (RA, Dec) = (18 35 45.74, +52 37 52.47) with an 90% error radius of 4''.4 (Troja et al. 2006a). The redshift of GRB 060502B is $z = 0.287$ (Bloom et al. 2007). FRB 190309A was detected by CHIME with a position of (RA, Dec) = $(278.96 \pm 0.23, 52.41 \pm 0.24)^4$ (The CHIME/FRB Collaboration et al. 2021). The angular separation between the two sources is 0.22° , less than the localization uncertainty of FRB 190309A by CHIME. FRB 190309A was detected 4694 days (~ 12.8 yr) after the GRB 060502B trigger. The observed total DM is 356.9 pc cm^{-3} and the extragalactic contribution $\text{DM}_E = \text{DM}_{\text{IGM}} + \text{DM}_{\text{host}}/(1+z)$ is 298.3 pc cm^{-3} (The CHIME/FRB Collaboration et al. 2021) when using the NE2001 model(Cordes & Lazio 2002). We estimate its redshift range to be $z \sim (0.23 \sim 0.54)$ (assuming a DM_{host} of 50 gives $z \sim (0.20 \sim 0.48)$), which covers the redshift of GRB 060502B.

To derive the significance of the association, we calculate the chance possibility of the putative GRB 060502B-FRB 190309A association by Monte Carlo (MC) simulation. The CHIME sky coverage is $2\pi(1 - \cos 101^\circ) = 7.48 \text{ sr}$, where 101° is the latitude range of the CHIME observation (RA: $0 - 360^\circ$, Dec: $-11^\circ - 90^\circ$) (The CHIME/FRB Collaboration et al. 2021). Due to the large sky coverage, the present FRB sample is dominated by the CHIME FRBs with 503 (483 one-off FRBs and 20 repeaters) out of 623 FRBs in the whole sample. Therefore, the MC simulation could be performed considering only the CHIME FRBs and the SGRBs within the CHIME sky coverage. There are $103/168 \approx 61.3\%$ SGRBs in our SGRB sample within the CHIME sky coverage. Finally, 503 CHIME FRBs and 103 SGRBs are used in this MC simulation.

We perform the MC simulation as follows: Based on the sky distributions of the observed 103 SGRBs and 503 FRBs, we generate 103 and 503 pseudo-SGRBs and FRBs within the CHIME sky coverage. The SGRBs are randomly sampled isotropically, while the FRBs follow the CHIME FRB distribution in the sky, as shown in Figure 2. For the simulated FRBs and SGRBs, we randomly assign each of them a localization error, observation time, and redshift taken from the actual data of the real FRBs and SGRBs⁵. It's important to note that the localization errors of CHIME FRBs are not uniform across the sky; they are notably better at lower declinations than at higher declinations. Therefore, we divide the sky into 3-degree declination bins and randomly select a real localization error from the CHIME FRBs within the corresponding bin based on the declination of the simulated FRB.

We perform 10^5 MC simulations (for each simulation 103 SGRBs and 503 FRBs are sampled) and calculate the chance probabilities as follows. For each simulation, we apply the three criteria mentioned above to select association candidates. We record the number of simulations in which there is at least one pair of pseudo-sources satisfying the criteria, denoted as N . The chance probability is then calculated as $P = N/10^5$. Considering only criterion I, we find a chance probability of 0.27. When criterion II is included, the chance probability is 0.21. With criterion III included, the chance probability is further reduced to 0.05.

3. IS GRB 060502B ASSOCIATED WITH FRB 190309A?

3.1. Host Galaxy

GRB 060502B triggered the *Swift*/BAT on 05 June 2006 (UT) at 17:24:41 (T_0), with $T_{90} = 0.131 \text{ s}$ (Troja et al. 2006b; Sato et al. 2006). The *Swift*/XRT and *Swift*/UVOT began to observe the X-ray and optical afterglow of GRB 060502B at 76 and 100 s after the *Swift*/BAT trigger, respectively (Troja et al. 2006b; Poole & Troja 2006). Many optical telescopes have carried out follow-up observations, e.g., MASTER optical telescopes (Lipunov et al. 2006), Xinglong 0.8m telescope (Zhai et al. 2006), Tautenburg 1.34m Schmidt telescope (Kann et al. 2006), AROMA optical telescope (Takahashi et al. 2006b,a), MDM 1.3m telescope (Halpern & Mirabal 2006b,a), Cassini telescope (Meurs et al. 2006), Gemini North telescope (Berger et al. 2006; Price et al. 2006) and MAO 1.5m telescope (Rumyantsev et al. 2006). No optical counterpart was found from several minutes to more than ten hours after the GRB 060502B trigger, and only a faint X-ray afterglow was detected by *Swift*/XRT.

The identification of the host galaxy of GRB 060502B has been studied in some previous works (Bloom et al. 2006a, 2007; Berger et al. 2007; Church et al. 2011, 2012). Bloom et al. (2007) proposed that a bright galaxy (referred to as G^*), situated south of the Swift/XRT localization of the GRB with an angular separation of 17.5 arcsec (approximately 73 kpc if assuming a redshift of $z \sim 0.287$), is the host galaxy of GRB 060502B (chance probability of 0.03). Church

⁴ <http://www.chime-frb.ca/catalog/FRB20190309A>

⁵ Only 36 SGRBs have redshift measurements, and we randomly draw one from these 36 redshifts for each pseudo-SGRB.

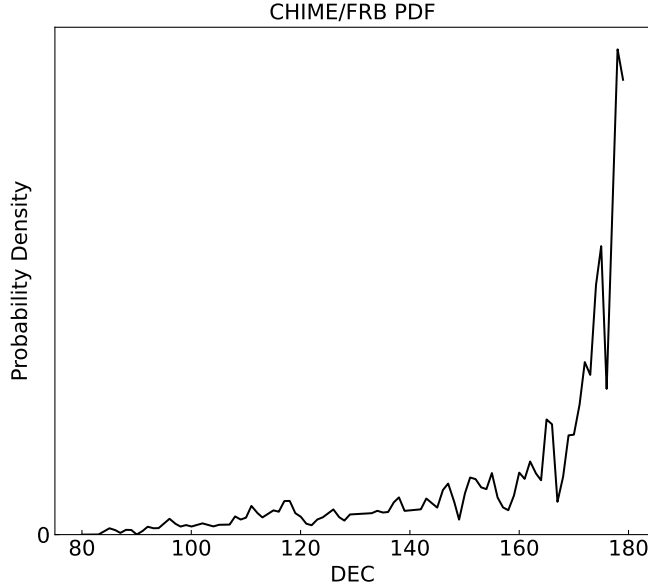


Figure 2. CHIME does not have a uniform exposure across the sky (The CHIME/FRB Collaboration et al. 2021). This plot shows the probability density distribution of the 503 CHIME FRBs as a function of declination, which is given by the relative number of FRBs in the $\text{DEC} \pm 1^\circ$ region divided by the corresponding solid angle.

et al. (2011) noted that such a large offset is inconsistent with the scenario that GRB 060502B originates from a compact binary merger in the galaxy. They suggest that either the precursor of GRB 060502B was a binary neutron star system that formed within a globular cluster inside G^* , giving this binary a large initial kick, or G^* is not the actual host galaxy of GRB 060502B. Except for the G^* , within 1 arcmin of the GRB 060502B position, we find no other possible host galaxy candidates for GRB 060502B with redshift measurements⁶. Furthermore, the results obtained from the relation between the spectral peak energy (E_p) and the isotropic gamma-ray energy ($E_{\gamma,\text{iso}}$), namely the *Amati-relation* (Amati et al. 2002; Wang et al. 2018), indicate that when adopting a redshift of G^* ($z = 0.287$ Zhang et al. (2009)) the GRB 060502B well lies within the SGRB's *Amati-relation*. Therefore, we also consider the bright galaxy G^* as the host galaxy for GRB 060502B.

The properties of the host environment (e.g., the offset from the host center, the star-formation rate (SFR), and the total stellar mass of the galaxy ($M_{\text{s,tot}}$)) may provide important clues for unveiling the origin of FRBs. Although the sample size of FRB host galaxies is still limited, some statistical analyses between FRB hosts and the host galaxies of other transient sources, e.g., SGRBs, core-collapse supernovae (CCSNe), Type Ia supernovae (SNe Ia), LGRBs, SLSNe, have been performed (Safarzadeh et al. 2020; Bhandari et al. 2020b; Heintz et al. 2020; Li & Zhang 2020; Mannings et al. 2021; Bochenek et al. 2021; Bhandari et al. 2022; Law et al. 2023). A majority of these works suggest that the host galaxies of SGRBs and CCSNe are similar to those of FRBs. In particular, Li & Zhang (2020) investigated 9 FRBs' hosts and suggested that the SFRs and the $M_{\text{s,tot}}$ of 8 of them are consistent with SGRBs. Bhandari et al. (2022) presented that the global properties (offset, SFR, $M_{\text{s,tot}}$) of FRB hosts are indistinguishable from those of the hosts of CCSNe and SGRBs.

To compare the host galaxy properties between the GRB 060502B (i.e., G^*) and the FRB population, we also demonstrate the offsets, SFRs, and $M_{\text{s,tot}}$ for 30 FRB hosts in Table 2 and Figure 3, including 17 FRBs from Bhandari et al. (2022), 11 FRBs from Law et al. (2023) and two possible hosts from Bhardwaj et al. (2021b) (FRB 181030A) and Bhandari et al. (2022) (FRB 181112A). The red lines denote the values for the G^* . As is shown in the figures, although the SFR of G^* falls well into the range of the FRB host galaxy population, the other two properties (offset and $M_{\text{s,tot}}$) are not consistent with those of FRBs, which do not support that G^* is a typical FRB host galaxy.

⁶ Here, we search for the candidates from the Extragalactic Database (NASA/IPAC Extragalactic Database (NED) 2019) and Sloan Digital Sky Survey <https://www.sdss.org/dr17/>.

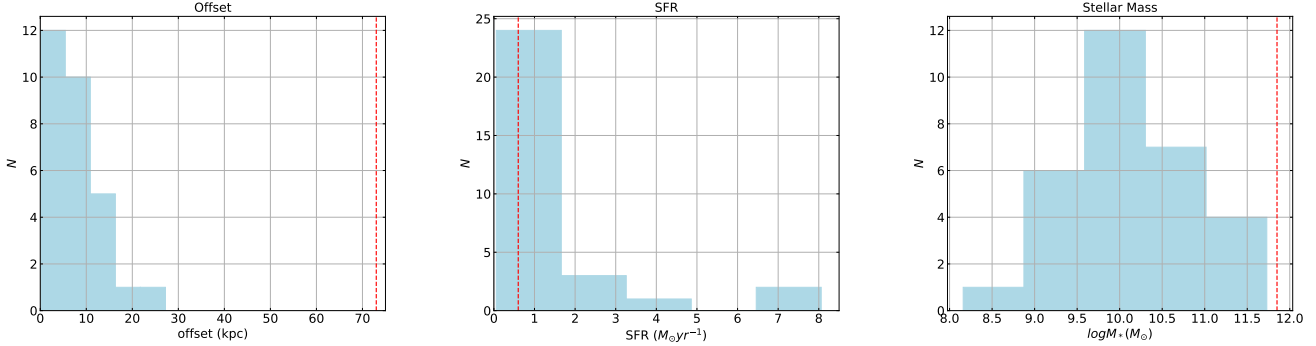


Figure 3. Distributions of offsets (left panel), host galaxy SFRs (middle panel), and stellar masses (right panel) for 30 FRBs (light blue region). The dashed red lines represent the values for GRB 060502B.

However, as mentioned above, if G^* is considered as the host galaxy of GRB 060502B, the possible born channel for this GRB is the merger of a BNS system formed in a GC of G^* (Church et al. 2011). Therefore, if FRB 190309A is associated with GRB 060502B, the FRB should also arise from this channel, which is not the same as the born channels of most of FRBs. One FRB that has a similar channel is the burst FRB 200120E. FRB 200120E could have arisen in a GC and been powered by a magnetar born from the merger of a compact binary system within the GC (Kirsten et al. 2022). Although the merger position of the progenitor of FRB 190309A is not identical to that of FRB 200120E, the sparse sample size currently does not allow us to tell whether G^* matches the host properties of this class of FRBs and thus cannot rule out the possibility that G^* serves as the host galaxy of FRB 190309A.

3.2. Dispersion Measure

DM_{host} can be resolved into three components, including DM_{src} , DM_{ISM} and DM_{halo} . They are the DMs contributed by the source environment, the interstellar medium (ISM), and the halo of the host galaxy, respectively. Here, we assume that GRB 060502B and FRB 190309A are associated, and we want to estimate whether the source environment of GRB 060502B can allow the FRB to escape and whether the observational DM_{host} of FRB 190309A can be explained by the host galaxy of GRB 060502B.

Since GRB 060502B is supposed to be from a BNS merger, its DM_{src} would be contributed by the ejecta of the BNS merger. The BNS merger ejecta is different from the CCSNe and has a higher velocity $v \sim (0.1 - 0.3)c$ and a lower mass $M \sim (10^{-4} - 10^{-2})M_{\odot}$. After the BNS merger, the DM_{src} can be derived as follows (Wang et al. 2020a),

$$\text{DM}_{\text{src}} = n_e \Delta R \simeq \frac{\eta Y_e M}{4\pi m_p (vt)^2} \simeq 0.17 \text{ pc cm}^{-3} \times \eta \left(\frac{Y_e}{0.2} \right) \left(\frac{M}{10^{-3} M_{\odot}} \right) \left(\frac{v}{0.2c} \right)^{-2} \left(\frac{t}{1 \text{ yr}} \right)^{-2} \quad (3)$$

where $n_e \simeq \eta Y_e M / [4\pi m_p (vt)^3]$ is the free electron density, $\Delta R \sim vt$ is the ejecta thickness, v is the speed of the ejecta, t is the elapsed time after the BNS merger, η is the ionization fraction, Y_e is the electron fraction, and M is the mass of the ejecta. The DM_{src} is derived to be $7.9 \times 10^{-4} \text{ pc cm}^{-3}$ using $t = 12.8$ yrs (the time difference between GRB 060502B and FRB 190309A). This indicates a clean source environment, which is thought to be a prerequisite for FRB escape if the magnetar acts as the central engine to power the FRB (Murase et al. 2016; Metzger et al. 2017; Margalit & Metzger 2018).

According to the redshift of GRB 060502B ($z = 0.287$), the $\overline{\text{DM}}_{\text{IGM}}$ can be estimated from equation (2), i.e. $\overline{\text{DM}}_{\text{IGM}} \simeq 245.2 \text{ pc cm}^{-3}$. We can derive that the DM_{host} is

$$\text{DM}_{\text{host}} = (1 + z)(\text{DM}_{\text{obs}} - \text{DM}_{\text{MW}} - \overline{\text{DM}}_{\text{IGM}}) \simeq 68.3 \text{ pc cm}^{-3} \quad (4)$$

where $\text{DM}_{\text{MW}} = 58.6 \text{ pc cm}^{-3}$ is the contribution from the Milky Way. Clearly, the DM_{src} ($\sim 7.9 \times 10^{-4} \text{ pc cm}^{-3}$) can be neglected. Meanwhile, due to the large offset between GRB 060502B and G^* , the DM_{ISM} part should also be neglected. Thus, the DM_{host} is mainly contributed by the DM_{halo} .

Following Church et al. (2011), we adopt the below profile to model the dark matter halo of G^* (Thomas et al. 2009),

$$\rho(r) = \frac{v_h^2}{4\pi G} \frac{3r_h^2 + r^2}{(r_h^2 + r^2)^2} \quad (5)$$

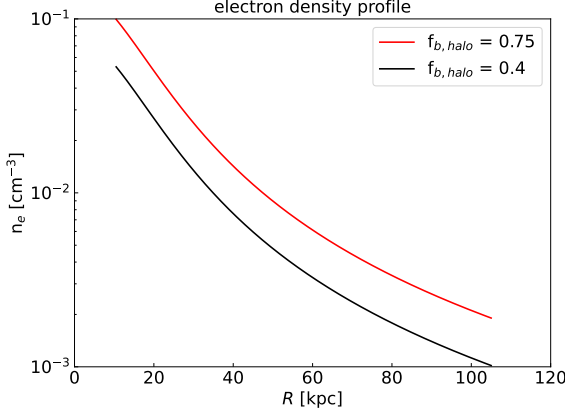


Figure 4. The electron number density as a function of halo radius in the halo of G^* .

where $r_h = 20.45$ kpc is the core radius of the halo, $v_h = 505.31 \text{ km s}^{-1}$ is the circular velocity at infinity and $G = 6.67 \times 10^{-11} \text{ m}^3 \text{ kg}^{-1} \text{ s}^{-2}$ is the gravitational constant. We take the halo mass from Church et al. (2011), i.e. $6.01 \times 10^{12} M_\odot$, which is enclosed within a spherical radius of $R_{\max} = 105$ kpc of the halo. We consider the simplest model for baryons in the halo, which are assumed to trace the underlying dark matter halo distribution (Prochaska & Zheng 2019). The baryon density in the halo is thus, $\rho_b(r) \propto f_{b,\text{halo}} \rho(r) \Omega_b / \Omega_m$, where the cosmic baryon fraction is $\Omega_b / \Omega_m \approx 0.158$ and $f_{b,\text{halo}}$ is the fraction of baryons existing in a halo form (i.e., excluding those portion in the form of ISM and stars). Here, we consider two values: (1) $f_{b,\text{halo}} = 0.75$, which assumes that $\approx 25\%$ of the baryons exist in the ISM, stars and their remnants (Fukugita et al. 1998). (2) $f_{b,\text{halo}} = 0.40$, which is a lower limit for a $\sim 10^{12} M_\odot$ halo found by Hafen et al. (2019).

The line of sight may travel through the G^* halo, and thus the DM contributed by the halo is

$$\text{DM}(x) = \int_0^x n_e dl. \quad (6)$$

The n_e is the free-electron number density in the halo, which can be estimated by (Prochaska & Zheng 2019)

$$n_e = \mu_e \frac{\rho_b}{m_p \mu_H} \quad (7)$$

where $\mu_H = 1.3$ the reduced mass (accounting for Helium) and $\mu_e = 1.167$ accounts for fully ionized Helium and Hydrogen. The electron number density distribution is shown in Figure 4. Considering that we don't know exactly the position of the source on the line of sight, the x in Eq. (6) could be $0 \leq x \leq 2\sqrt{R_{\max}^2 - R_\perp^2} = 151$ kpc (where $R_\perp = 73$ kpc is the impact parameter) and we can only estimate the DM_{halo} range corresponding to x varying from 0 to 151 kpc. Therefore, we obtain the range of DM_{halo} of $0 - 470 \text{ pc cm}^{-3}$ (for $f_{b,\text{halo}} = 0.75$) or $0 - 250 \text{ pc cm}^{-3}$ (for $f_{b,\text{halo}} = 0.4$). Although the DM_{halo} result is affected by the profile model of the galaxy halo (one can see Figure 1 in Prochaska & Zheng (2019), which shows the DM_{halo} results for different halo profiles; see also Cook et al. (2023) for a newly developed model of the Galactic electron halo), at least for the profile considered in this paper [Eq. (5)], the DM_{host} of FRB 190309A (68.3 pc cm^{-3}) is compatible with the possibility that G^* is the host galaxy.

3.3. Optical Depth and Time Delay

In addition, the ejecta surrounding the newborn magnetar could affect the observational signature of FRBs. We here consider the free-free optical depth due to the ejecta of the BNS merger. When the ejecta is transparent to the FRB, the free-free optical depth should be less than 1. We can derive the free-free optical depth with (Wang et al. 2020a)

$$\begin{aligned} \tau_{\text{ff}} = \alpha_{\text{ff}} \Delta R &\simeq (0.018 T_{\text{eje}}^{-3/2} Z^2 n_e n_i \nu^{-2} \bar{g}_{\text{ff}}) \Delta R = 2.7 \times 10^{-8} \\ &\times \eta^2 \left(\frac{Y_e}{0.2} \right)^2 \left(\frac{M}{10^{-3} M_\odot} \right)^2 \left(\frac{T_{\text{eje}}}{10^4 \text{ K}} \right)^{-3/2} \left(\frac{\nu}{1 \text{ GHz}} \right)^{-2} \left(\frac{v}{0.2 \text{ c}} \right)^{-5} \left(\frac{t}{1 \text{ yr}} \right)^{-5} \end{aligned} \quad (8)$$

where n_e and n_i are the number densities of electrons and ions, respectively, and $n_e \sim n_i$ and $Z \sim 1$ are assumed in the ejecta that is a fully ionized hydrogen-dominated composition, T_{eje} is the ejecta temperature, $\bar{g}_{\text{ff}} \sim 1$ is the Gaunt factor. The calculated result suggests that the FRB could be detected a few weeks after the BNS merger. Therefore, the optical depth allows the FRB 190309A to escape the source environment of GRB 060502B.

The FRB emitted from a magnetar has been proposed to be due to magnetospheric activities. When the magnetar magnetosphere is triggered by a crust fracturing, the magnetic energy in the crust will be released and converted into particle energy and radiation, and an FRB is emitted (Kumar & Bošnjak 2020; Wadiasingh & Timokhin 2019; Dehman et al. 2020; Lu et al. 2020). In this picture, as long as the magnetar exists, it is possible to produce FRBs through a crust fracturing, and the time of the crust fracturing is extremely uncertain during the existence of the magnetar. Here, we estimate the timescale for the existence of the magnetar (i.e., the timescale of magnetic field decay). The magnetic field in the crust would decay via the Ohmic dissipation and the evolution of the magnetic field can be approximated by $dB/dt \simeq -AB$ (Yang & Zhang 2021) with $A = 10^{18} \text{ G}^{-1} \text{ yr}^{-1}$ (Colpi et al. 2000). Then the typical timescale of magnetic field decay is (Yang & Zhang 2021)

$$\tau_B = \frac{1}{AB_0} = 10^4 \text{ yr} \left(\frac{B_0}{10^{14} \text{ G}} \right)^{-1} \quad (9)$$

where B_0 is the initial magnetic field. One can see that the timescale of magnetic field decay (and thus the time delay of the FRB) could be 10^4 years for $B_0 = 10^{14}$ G. For example, FRB 200428 may be released by the magnetospheric activities of a Galactic magnetar with an age of approximately 10^4 yrs (Bochenek et al. 2020; Wang et al. 2021). Therefore, the relatively large time span (~ 12.8 yr) between GRB 060502B and FRB 190309A is also compatible with the model.

3.4. Energy Budget

Although the central engine of FRBs is generally considered to be a magnetar, the exact process for the generation of FRBs differs in different models. For instance, FRBs could be generated by synchrotron maser in relativistic shocks driven by the magnetar flares (Lyubarsky 2014; Metzger et al. 2019; Beloborodov 2020), by the curvature radiation in the magnetosphere (Lu et al. 2020), by the magnetic reconnection of external magnetosphere (Lyubarsky 2020), or by the inverse Compton scattering in the magnetosphere (Zhang 2022). Here, rather than going into the details of any of the above models, we consider only a conservative estimate of the magnetic field of the magnetar, since for all of these models FRBs are essentially driven by the magnetic energy of the magnetar.

Within this picture, we try to calculate whether the magnetar could be used as the central engine of FRB 190309A. FRB 190309A has a duration of $\Delta t \sim 1.97$ ms, a flux of $S_{\nu,p} \sim 0.39$ Jy and a fluence of $f_\nu \sim 0.72$ Jy ms at $\nu_c \sim 468$ MHz. Assuming that FRB 190309A is associated with GRB 060502B, one can derive the luminosity distance as $D_L \sim 1.52$ Gpc according to the redshift of GRB 060502B ($z \sim 0.287$). The luminosity and isotropic energy of FRB 190309A can be calculated as $L_p \simeq 4\pi D_L^2 S_{\nu,p} \nu_c \simeq 5.1 \times 10^{41}$ erg s $^{-1}$ and $E_{\text{FRB}} \simeq 4\pi D_L^2 f_\nu \nu_c / (1+z) \simeq 7.3 \times 10^{38}$ erg. If this energy is provided by the magnetic energy of the magnetar, one can place a constraint on the strength of the surface polar cap magnetic field of the underlying magnetar.

The emission radius can be approximately estimated as $r_e \sim c\Delta t \simeq 5.91 \times 10^7$ cm, which is consistent with the predicted emission radius of the magnetar that produced the FRB, i.e., a few $\times 10 R_{\text{NS}} \sim 10^7$ cm (Lyutikov 2021). The magnetic field strength at r_e should satisfy

$$\frac{B_e^2}{8\pi} \left(\frac{4\pi}{3} r_e^3 \right) \geq E_{\text{FRB}}, \quad (10)$$

where $B_e = B_p (r_e/R)^{-3}$ (Wang et al. 2020b) and B_p , $R (\sim 10^6$ cm) are the magnetic field strength of the surface polar cap and typical radius of the magnetar, respectively. Therefore, the observation of FRB 190309A demands that the magnetic field strength of the surface polar cap is

$$B_p \geq \left(\frac{6Er_e^3}{R^6} \right)^{1/2} \simeq 3 \times 10^{13} \text{ G}, \quad (11)$$

which is indeed consistent with a magnetar central engine.

4. SUMMARY

In this work, we systematically search for possible associations between SGRBs and FRBs based on a sample of 623 FRBs (601 one-off bursts and 22 repeaters) and 168 SGRBs. We find that FRB 190309A is spatially coincident with GRB 060502B. Moreover, GRB 060502B occurred earlier than FRB 190309A, and its redshift is consistent with the range of the distance derived from the DM of FRB 190309A. Considering the observational information such as spatial location, time of occurrence, and redshift, we obtain a chance probability of the association of ~ 0.05 .

Considering the statistical significance is not high enough ($< 3\sigma$) to claim a reliable association between GRB 060502B and FRB 190309A, we further investigate if there is any other evidence to support the physical association between them. We find that the (candidate) host galaxy of GRB 060502B, G^* , has an SFR similar to the hosts of the FRB population, but for another two host properties we have investigated (i.e., the offset from the host center and the total stellar mass of the galaxy), the G^* ones do not coincide with the distributions of 19 FRBs. However, considering that FRB 190309A may have a different born channel of its underlying magnetar from these FRBs, it may not be enough to exclude the association between FRB 190309A and GRB 060502B on this basis. In addition, adopting the redshift of GRB 060502B, we estimate that FRB 190309A has a $DM_{host} \simeq 68.3 \text{ pc cm}^{-3}$, which is able to be contributed by the (candidate) host galaxy G^* of GRB 060502B. We also derive the free-free optical depth around the source and find it allows the FRB to be detectable. Finally, adopting the redshift of GRB 060502B, we obtain an isotropic energy of $E_{\text{FRB}} \sim 7.3 \times 10^{38} \text{ erg}$ for FRB190309A; accordingly, the required surface magnetic field to power FRB 190309A is $B_p \geq 3 \times 10^{13} \text{ G}$, which is also consistent with the typical magnetic field of the SGRB magnetars. These results indicate that a physical association between GRB 060502B and FRB 190309A is feasible.

Overall, in this paper we do not find a reliable SGRB counterpart that is associated with FRBs; one possible FRB-SGRB association is between GRB 060502B and FRB 190309A, but it has a relatively large chance probability ($p \sim 0.05$). Even though, considering that this is at present the only pair of FRB and GRB that are spatially associated, it is still worthy of our attention. We therefore detailedly examine the possibility of their physical association from the aspects of the host galaxy, the DM, the energy budget, etc., and find that all of these could not exclude the possibility of their association. For this reason, we suggest that GRB 060502B/FRB 190309A pair is still a promising case of FRB-SGRB association that is worth further studying.

ACKNOWLEDGEMENTS

We acknowledge the use of public data from the *Swift*, CHIME, GCN, TNS and frbhosts data archive. This work is supported by the National Natural Science Foundation of China (Nos. U1938201, 12133003, U1731239, 12203013), the Guangxi Science Foundation (grants 2018GXNSFGA281007, 2017AD22006, 2021AC19263).

REFERENCES

- Abbott, B. P., Abbott, R., Abbott, T. D., et al. 2017a, PhRvL, 119, 161101, doi: [10.1103/PhysRevLett.119.161101](https://doi.org/10.1103/PhysRevLett.119.161101)
- . 2017b, ApJL, 848, L12, doi: [10.3847/2041-8213/aa91c9](https://doi.org/10.3847/2041-8213/aa91c9)
- Aggarwal, K., Budavári, T., Deller, A. T., et al. 2021, ApJ, 911, 95, doi: [10.3847/1538-4357/abe8d2](https://doi.org/10.3847/1538-4357/abe8d2)
- Ahumada, R., Prieto, C. A., Almeida, A., et al. 2020, ApJS, 249, 3, doi: [10.3847/1538-4365/ab929e](https://doi.org/10.3847/1538-4365/ab929e)
- Amati, L., Frontera, F., Tavani, M., et al. 2002, A&A, 390, 81, doi: [10.1051/0004-6361:20020722](https://doi.org/10.1051/0004-6361:20020722)
- Anderson, G. E., Hancock, P. J., Rowlinson, A., et al. 2021, PASA, 38, e026, doi: [10.1017/pasa.2021.15](https://doi.org/10.1017/pasa.2021.15)
- Anderson, M. M., Hallinan, G., Eastwood, M. W., et al. 2018, ApJ, 864, 22, doi: [10.3847/1538-4357/aad2d7](https://doi.org/10.3847/1538-4357/aad2d7)
- Bannister, K. W., Murphy, T., Gaensler, B. M., & Reynolds, J. E. 2012, ApJ, 757, 38, doi: [10.1088/0004-637X/757/1/38](https://doi.org/10.1088/0004-637X/757/1/38)
- Bannister, K. W., Deller, A. T., Phillips, C., et al. 2019, Science, 365, 565, doi: [10.1126/science.aaw5903](https://doi.org/10.1126/science.aaw5903)
- Barbier, L., Barthelmy, S. D., Cummings, J., et al. 2007, GRB Coordinates Network, 6623, 1
- Barthelmy, S. D., Chincarini, G., Burrows, D. N., et al. 2005, Nature, 438, 994, doi: [10.1038/nature04392](https://doi.org/10.1038/nature04392)
- Barthelmy, S. D., Baumgartner, W. H., Cummings, J. R., et al. 2009, GRB Coordinates Network, 9494, 1
- Barthelmy, S. D., Cannizzo, J. K., Cummings, J. R., et al. 2017, GRB Coordinates Network, 21981, 1
- Beardmore, A. P., Page, K. L., Palmer, D. M., & Ukwatta, T. N. 2015, GRB Coordinates Network, 17743, 1
- Beloborodov, A. M. 2017, ApJL, 843, L26, doi: [10.3847/2041-8213/aa78f3](https://doi.org/10.3847/2041-8213/aa78f3)
- . 2020, ApJ, 896, 142, doi: [10.3847/1538-4357/ab83eb](https://doi.org/10.3847/1538-4357/ab83eb)
- Beloborodov, A. M., & Thompson, C. 2007, ApJ, 657, 967, doi: [10.1086/508917](https://doi.org/10.1086/508917)

- Berger, E. 2014, ARA&A, 52, 43, doi: [10.1146/annurev-astro-081913-035926](https://doi.org/10.1146/annurev-astro-081913-035926)
- Berger, E., Cenko, S. B., & Rau, A. 2006, GRB Coordinates Network, 5071, 1
- Berger, E., Fox, D. B., Price, P. A., et al. 2007, ApJ, 664, 1000, doi: [10.1086/518762](https://doi.org/10.1086/518762)
- Bhandari, S., Bannister, K. W., Lenc, E., et al. 2020a, ApJL, 901, L20, doi: [10.3847/2041-8213/abb462](https://doi.org/10.3847/2041-8213/abb462)
- Bhandari, S., Sadler, E. M., Prochaska, J. X., et al. 2020b, ApJL, 895, L37, doi: [10.3847/2041-8213/ab672e](https://doi.org/10.3847/2041-8213/ab672e)
- Bhandari, S., Heintz, K. E., Aggarwal, K., et al. 2022, AJ, 163, 69, doi: [10.3847/1538-3881/ac3aecc](https://doi.org/10.3847/1538-3881/ac3aecc)
- Bhardwaj, M., Gaensler, B. M., Kaspi, V. M., et al. 2021a, ApJL, 910, L18, doi: [10.3847/2041-8213/abeaa6](https://doi.org/10.3847/2041-8213/abeaa6)
- Bhardwaj, M., Kirichenko, A. Y., Michilli, D., et al. 2021b, ApJL, 919, L24, doi: [10.3847/2041-8213/ac223b](https://doi.org/10.3847/2041-8213/ac223b)
- Bloom, J. S., Kulkarni, S. R., & Djorgovski, S. G. 2002, AJ, 123, 1111, doi: [10.1086/338893](https://doi.org/10.1086/338893)
- Bloom, J. S., Perley, D., Kocevski, D., et al. 2006a, GRB Coordinates Network, 5238, 1
- Bloom, J. S., Prochaska, J. X., Pooley, D., et al. 2006b, ApJ, 638, 354, doi: [10.1086/498107](https://doi.org/10.1086/498107)
- Bloom, J. S., Perley, D. A., Chen, H. W., et al. 2007, ApJ, 654, 878, doi: [10.1086/509114](https://doi.org/10.1086/509114)
- Bochenek, C. D., Ravi, V., Belov, K. V., et al. 2020, Nature, 587, 59, doi: [10.1038/s41586-020-2872-x](https://doi.org/10.1038/s41586-020-2872-x)
- Bochenek, C. D., Ravi, V., & Dong, D. 2021, ApJL, 907, L31, doi: [10.3847/2041-8213/abd634](https://doi.org/10.3847/2041-8213/abd634)
- Briggs, M. S., Paciesas, W. S., Pendleton, G. N., et al. 1996, ApJ, 459, 40, doi: [10.1086/176867](https://doi.org/10.1086/176867)
- Butler, N., Ricker, G., Atteia, J. L., et al. 2005, GRB Coordinates Network, 3570, 1
- Caleb, M., Flynn, C., Bailes, M., et al. 2016, MNRAS, 458, 708, doi: [10.1093/mnras/stw175](https://doi.org/10.1093/mnras/stw175)
- Cannizzo, K. C., Barbier, L. M., Barthelmy, S. D., et al. 2006, GRB Coordinates Network, 5904, 1
- Casentini, C., Verrecchia, F., Tavani, M., et al. 2020, ApJL, 890, L32, doi: [10.3847/2041-8213/ab720a](https://doi.org/10.3847/2041-8213/ab720a)
- Champion, D. J., Petroff, E., Kramer, M., et al. 2016, MNRAS, 460, L30, doi: [10.1093/mnrasl/slw069](https://doi.org/10.1093/mnrasl/slw069)
- Chatterjee, S., Law, C. J., Wharton, R. S., et al. 2017, Nature, 541, 58, doi: [10.1038/nature20797](https://doi.org/10.1038/nature20797)
- Chen, X., Wang, W., & Tong, H. 2021, Journal of High Energy Astrophysics, 31, 1, doi: [10.1016/j.jheap.2021.04.002](https://doi.org/10.1016/j.jheap.2021.04.002)
- Cheng, Y., Zhang, G. Q., & Wang, F. Y. 2020, MNRAS, 491, 1498, doi: [10.1093/mnras/stz3085](https://doi.org/10.1093/mnras/stz3085)
- CHIME/FRB Collaboration, Andersen, B. C., Bandura, K., et al. 2019, ApJL, 885, L24, doi: [10.3847/2041-8213/ab4a80](https://doi.org/10.3847/2041-8213/ab4a80)
- CHIME/FRB Collaboration, Andersen, B. C., Bandura, K. M., et al. 2020, Nature, 587, 54, doi: [10.1038/s41586-020-2863-y](https://doi.org/10.1038/s41586-020-2863-y)
- Chittidi, J. S., Simha, S., Mannings, A., et al. 2021, ApJ, 922, 173, doi: [10.3847/1538-4357/ac2818](https://doi.org/10.3847/1538-4357/ac2818)
- Church, R. P., Levan, A. J., Davies, M. B., & Tanvir, N. 2011, MNRAS, 413, 2004, doi: [10.1111/j.1365-2966.2011.18277.x](https://doi.org/10.1111/j.1365-2966.2011.18277.x)
- . 2012, Memorie della Societa Astronomica Italiana Supplementi, 21, 104. <https://arxiv.org/abs/1110.4209>
- Colpi, M., Geppert, U., & Page, D. 2000, ApJL, 529, L29, doi: [10.1086/312448](https://doi.org/10.1086/312448)
- Cook, A. M., Bhardwaj, M., Gaensler, B. M., et al. 2023, ApJ, 946, 58, doi: [10.3847/1538-4357/acbbd0](https://doi.org/10.3847/1538-4357/acbbd0)
- Cook, G. B., Shapiro, S. L., & Teukolsky, S. A. 1994, ApJ, 424, 823, doi: [10.1086/173934](https://doi.org/10.1086/173934)
- Cordes, J. M., & Chatterjee, S. 2019, ARA&A, 57, 417, doi: [10.1146/annurev-astro-091918-104501](https://doi.org/10.1146/annurev-astro-091918-104501)
- Cordes, J. M., & Lazio, T. J. W. 2002, arXiv e-prints, astro. <https://arxiv.org/abs/astro-ph/0207156>
- Cordes, J. M., Ocker, S. K., & Chatterjee, S. 2021, arXiv e-prints, arXiv:2108.01172. <https://arxiv.org/abs/2108.01172>
- Cunningham, V., Cenko, S., Burns, E., et al. 2020, in American Astronomical Society Meeting Abstracts, Vol. 235, American Astronomical Society Meeting Abstracts #235, 439.03
- Cunningham, V., Cenko, S. B., Burns, E., et al. 2019, ApJ, 879, 40, doi: [10.3847/1538-4357/ab2235](https://doi.org/10.3847/1538-4357/ab2235)
- Cunningham, V. A., & Cenko, B. 2018, in American Astronomical Society Meeting Abstracts, Vol. 231, American Astronomical Society Meeting Abstracts #231, 243.08
- Curtin, A. P., Tendulkar, S. P., Josephy, A., et al. 2022, arXiv e-prints, arXiv:2208.00803. <https://arxiv.org/abs/2208.00803>
- Dai, Z. G., Wang, J. S., Wu, X. F., & Huang, Y. F. 2016, ApJ, 829, 27, doi: [10.3847/0004-637X/829/1/27](https://doi.org/10.3847/0004-637X/829/1/27)
- Day, C. K., Deller, A. T., James, C. W., et al. 2021, PASA, 38, e050, doi: [10.1017/pasa.2021.40](https://doi.org/10.1017/pasa.2021.40)
- Dehman, C., Viganò, D., Rea, N., et al. 2020, ApJL, 902, L32, doi: [10.3847/2041-8213/abbd9](https://doi.org/10.3847/2041-8213/abbd9)
- DeLaunay, J. J., Fox, D. B., Murase, K., et al. 2016, ApJL, 832, L1, doi: [10.3847/2041-8205/832/1/L1](https://doi.org/10.3847/2041-8205/832/1/L1)
- D'Elia, V., Barthelmy, S. D., Beardmore, A. P., et al. 2011, GRB Coordinates Network, 12578, 1
- Deng, C.-M., Wei, J.-J., & Wu, X.-F. 2019, Journal of High Energy Astrophysics, 23, 1, doi: [10.1016/j.jheap.2019.05.001](https://doi.org/10.1016/j.jheap.2019.05.001)

- Deng, C.-M., Zhong, S.-Q., & Dai, Z.-G. 2021, ApJ, 922, 98, doi: [10.3847/1538-4357/ac30db](https://doi.org/10.3847/1538-4357/ac30db)
- Deng, W., & Zhang, B. 2014, ApJL, 783, L35, doi: [10.1088/2041-8205/783/2/L35](https://doi.org/10.1088/2041-8205/783/2/L35)
- Dessenne, C. A. C., Green, D. A., Warner, P. J., et al. 1996, MNRAS, 281, 977, doi: [10.1093/mnras/281.3.977](https://doi.org/10.1093/mnras/281.3.977)
- Du, S. 2020, ApJ, 901, 75, doi: [10.3847/1538-4357/abaf4d](https://doi.org/10.3847/1538-4357/abaf4d)
- Falcke, H., & Rezzolla, L. 2014, A&A, 562, A137, doi: [10.1051/0004-6361/201321996](https://doi.org/10.1051/0004-6361/201321996)
- Faucher-Giguère, C.-A., Kereš, D., & Ma, C.-P. 2011, MNRAS, 417, 2982, doi: [10.1111/j.1365-2966.2011.19457.x](https://doi.org/10.1111/j.1365-2966.2011.19457.x)
- Fermi Gbm Team, & Likely Short Grb, T. D. O. A. 2021, GRB Coordinates Network, 30248, 1
- Fletcher, C., & Fermi-GBM Team. 2021, GRB Coordinates Network, 29536, 1
- Fong, W., & Berger, E. 2013, ApJ, 776, 18, doi: [10.1088/0004-637X/776/1/18](https://doi.org/10.1088/0004-637X/776/1/18)
- Fong, W., Berger, E., & Fox, D. B. 2010, ApJ, 708, 9, doi: [10.1088/0004-637X/708/1/9](https://doi.org/10.1088/0004-637X/708/1/9)
- Fong, W., Berger, E., Chornock, R., et al. 2013, ApJ, 769, 56, doi: [10.1088/0004-637X/769/1/56](https://doi.org/10.1088/0004-637X/769/1/56)
- Fox, D. B., Frail, D. A., Price, P. A., et al. 2005, Nature, 437, 845, doi: [10.1038/nature04189](https://doi.org/10.1038/nature04189)
- Fukugita, M., Hogan, C. J., & Peebles, P. J. E. 1998, ApJ, 503, 518, doi: [10.1086/306025](https://doi.org/10.1086/306025)
- Gao, H., Zhang, B., & Lü, H.-J. 2016, PhRvD, 93, 044065, doi: [10.1103/PhysRevD.93.044065](https://doi.org/10.1103/PhysRevD.93.044065)
- Gehrels, N., Sarazin, C. L., O'Brien, P. T., et al. 2005, Nature, 437, 851, doi: [10.1038/nature04142](https://doi.org/10.1038/nature04142)
- Geng, J., Li, B., & Huang, Y. 2021, The Innovation, 2, 100152, doi: [10.1016/j.xinn.2021.100152](https://doi.org/10.1016/j.xinn.2021.100152)
- Gohar, N., & Flynn, C. 2022, MNRAS, 509, 5265, doi: [10.1093/mnras/stab3349](https://doi.org/10.1093/mnras/stab3349)
- Goldstein, A., Veres, P., Burns, E., et al. 2017, ApJL, 848, L14, doi: [10.3847/2041-8213/aa8f41](https://doi.org/10.3847/2041-8213/aa8f41)
- Golenetskii, S., Aptekar, R., Mazets, E., et al. 2008, GRB Coordinates Network, 8676, 1
- Gourdji, K., Rowlinson, A., Wijers, R. A. M. J., & Goldstein, A. 2020, MNRAS, 497, 3131, doi: [10.1093/mnras/staa2128](https://doi.org/10.1093/mnras/staa2128)
- Grupe, D., Cummings, J. R., Gronwall, C., et al. 2009, GRB Coordinates Network, 9945, 1
- Hafen, Z., Faucher-Giguère, C.-A., Anglés-Alcázar, D., et al. 2019, MNRAS, 488, 1248, doi: [10.1093/mnras/stz1773](https://doi.org/10.1093/mnras/stz1773)
- Hallinan, G., Dong, D., & Ravi, V. 2019, The Astronomer's Telegram, 13018, 1
- Halpern, J. P., & Mirabal, N. 2006a, GRB Coordinates Network, 5072, 1
- . 2006b, GRB Coordinates Network, 5066, 1
- Hardy, L. K., Dhillon, V. S., Spitler, L. G., et al. 2017, MNRAS, 472, 2800, doi: [10.1093/mnras/stx2153](https://doi.org/10.1093/mnras/stx2153)
- Heintz, K. E., Prochaska, J. X., Simha, S., et al. 2020, ApJ, 903, 152, doi: [10.3847/1538-4357/abb6fb](https://doi.org/10.3847/1538-4357/abb6fb)
- Hut, P., McMillan, S., Goodman, J., et al. 1992, PASP, 104, 981, doi: [10.1086/133085](https://doi.org/10.1086/133085)
- Ioka, K., & Zhang, B. 2020, ApJL, 893, L26, doi: [10.3847/2041-8213/ab83fb](https://doi.org/10.3847/2041-8213/ab83fb)
- Israel, G. L., Esposito, P., Rea, N., et al. 2016, MNRAS, 457, 3448, doi: [10.1093/mnras/stw008](https://doi.org/10.1093/mnras/stw008)
- James, C. W., Anderson, G. E., Wen, L., et al. 2019, MNRAS, 489, L75, doi: [10.1093/mnras/slz129](https://doi.org/10.1093/mnras/slz129)
- Kann, D. A., Klose, S., & Ferrero, P. 2006, GRB Coordinates Network, 5062, 1
- Kaplan, D. L., Rowlinson, A., Bannister, K. W., et al. 2015, ApJL, 814, L25, doi: [10.1088/2041-8205/814/2/L25](https://doi.org/10.1088/2041-8205/814/2/L25)
- Kashiyama, K., Ioka, K., & Mészáros, P. 2013, ApJL, 776, L39, doi: [10.1088/2041-8205/776/2/L39](https://doi.org/10.1088/2041-8205/776/2/L39)
- Katz, J. I. 2016, ApJ, 826, 226, doi: [10.3847/0004-637X/826/2/226](https://doi.org/10.3847/0004-637X/826/2/226)
- Keating, L. C., & Pen, U.-L. 2020, MNRAS, 496, L106, doi: [10.1093/mnrasl/slaa095](https://doi.org/10.1093/mnrasl/slaa095)
- Kirsten, F., Marcote, B., Nimmo, K., et al. 2022, Nature, 602, 585, doi: [10.1038/s41586-021-04354-w](https://doi.org/10.1038/s41586-021-04354-w)
- Kouveliotou, C., Meegan, C. A., Fishman, G. J., et al. 1993, ApJL, 413, L101, doi: [10.1086/186969](https://doi.org/10.1086/186969)
- Krimm, H., Barbier, L., Barthelmy, S., et al. 2005, GRB Coordinates Network, 3667, 1
- . 2006, GRB Coordinates Network, 5704, 1
- Kulkarni, S. R., Ofek, E. O., Neill, J. D., Zheng, Z., & Juric, M. 2014, ApJ, 797, 70, doi: [10.1088/0004-637X/797/1/70](https://doi.org/10.1088/0004-637X/797/1/70)
- Kumar, P., & Bošnjak, Ž. 2020, MNRAS, 494, 2385, doi: [10.1093/mnras/staa774](https://doi.org/10.1093/mnras/staa774)
- Kumar, P., & Zhang, B. 2015, PhR, 561, 1, doi: [10.1016/j.physrep.2014.09.008](https://doi.org/10.1016/j.physrep.2014.09.008)
- Law, C. J., Butler, B. J., Prochaska, J. X., et al. 2020, ApJ, 899, 161, doi: [10.3847/1538-4357/aba4ac](https://doi.org/10.3847/1538-4357/aba4ac)
- Law, C. J., Sharma, K., Ravi, V., et al. 2023, arXiv e-prints, arXiv:2307.03344, doi: [10.48550/arXiv.2307.03344](https://doi.org/10.48550/arXiv.2307.03344)
- Li, C. K., Lin, L., Xiong, S. L., et al. 2021, Nature Astronomy, 5, 378, doi: [10.1038/s41550-021-01302-6](https://doi.org/10.1038/s41550-021-01302-6)
- Li, L., Li, Q.-C., Zhong, S.-Q., et al. 2022, arXiv e-prints, arXiv:2203.06994. <https://arxiv.org/abs/2203.06994>
- Li, Y., & Zhang, B. 2020, ApJL, 899, L6, doi: [10.3847/2041-8213/aba907](https://doi.org/10.3847/2041-8213/aba907)
- Li, Y., Zhang, B., Nagamine, K., & Shi, J. 2019, ApJL, 884, L26, doi: [10.3847/2041-8213/ab3e41](https://doi.org/10.3847/2041-8213/ab3e41)
- Liang, E., & Zhang, B. 2005, ApJ, 633, 611, doi: [10.1086/491594](https://doi.org/10.1086/491594)

- Liang, Y.-F., Xia, Z.-Q., Duan, K.-K., et al. 2017, PhRvD, 95, 063531, doi: [10.1103/PhysRevD.95.063531](https://doi.org/10.1103/PhysRevD.95.063531)
- Lin, H., & Totani, T. 2020, MNRAS, 498, 2384, doi: [10.1093/mnras/staa2418](https://doi.org/10.1093/mnras/staa2418)
- Lipunov, V., Kornilov, V., Tyurina, N., et al. 2006, GRB Coordinates Network, 5056, 1
- Liu, H.-Y., Wang, X.-G., Xin, L.-P., et al. 2022, Research in Astronomy and Astrophysics, 22, 065002, doi: [10.1088/1674-4527/ac65e6](https://doi.org/10.1088/1674-4527/ac65e6)
- Liu, T., Romero, G. E., Liu, M.-L., & Li, A. 2016, ApJ, 826, 82, doi: [10.3847/0004-637X/826/1/82](https://doi.org/10.3847/0004-637X/826/1/82)
- Lorimer, D. R., Bailes, M., McLaughlin, M. A., Narkevic, D. J., & Crawford, F. 2007, Science, 318, 777, doi: [10.1126/science.1147532](https://doi.org/10.1126/science.1147532)
- Lü, H.-J., Lan, L., & Liang, E.-W. 2019, ApJ, 871, 54, doi: [10.3847/1538-4357/aaef71d](https://doi.org/10.3847/1538-4357/aaef71d)
- Lü, H.-J., Zhang, B., Lei, W.-H., Li, Y., & Lasky, P. D. 2015, ApJ, 805, 89, doi: [10.1088/0004-637X/805/2/89](https://doi.org/10.1088/0004-637X/805/2/89)
- Lu, W., & Kumar, P. 2016, MNRAS, 461, L122, doi: [10.1093/mnrasl/slw113](https://doi.org/10.1093/mnrasl/slw113)
- . 2018, MNRAS, 477, 2470, doi: [10.1093/mnras/sty716](https://doi.org/10.1093/mnras/sty716)
- Lu, W., Kumar, P., & Zhang, B. 2020, MNRAS, 498, 1397, doi: [10.1093/mnras/staa2450](https://doi.org/10.1093/mnras/staa2450)
- Luo, R., Wang, B. J., Men, Y. P., et al. 2020, Nature, 586, 693, doi: [10.1038/s41586-020-2827-2](https://doi.org/10.1038/s41586-020-2827-2)
- Lyubarsky, Y. 2014, MNRAS, 442, L9, doi: [10.1093/mnrasl/slu046](https://doi.org/10.1093/mnrasl/slu046)
- . 2020, ApJ, 897, 1, doi: [10.3847/1538-4357/ab97b5](https://doi.org/10.3847/1538-4357/ab97b5)
- Lyutikov, M. 2021, arXiv e-prints, arXiv:2110.08435. <https://arxiv.org/abs/2110.08435>
- Macquart, J. P., Prochaska, J. X., McQuinn, M., et al. 2020, Nature, 581, 391, doi: [10.1038/s41586-020-2300-2](https://doi.org/10.1038/s41586-020-2300-2)
- Mahony, E. K., Ekers, R. D., Macquart, J.-P., et al. 2018, ApJL, 867, L10, doi: [10.3847/2041-8213/aae7cb](https://doi.org/10.3847/2041-8213/aae7cb)
- Mannings, A. G., Fong, W.-f., Simha, S., et al. 2021, ApJ, 917, 75, doi: [10.3847/1538-4357/abff56](https://doi.org/10.3847/1538-4357/abff56)
- Mao, J., Baumgartner, W. H., Burrows, D. N., et al. 2008, GRB Coordinates Network, 7665, 1
- Marcote, B., Paragi, Z., Hessels, J. W. T., et al. 2017, ApJL, 834, L8, doi: [10.3847/2041-8213/834/2/L8](https://doi.org/10.3847/2041-8213/834/2/L8)
- Marcote, B., Nimmo, K., Hessels, J. W. T., et al. 2020, Nature, 577, 190, doi: [10.1038/s41586-019-1866-z](https://doi.org/10.1038/s41586-019-1866-z)
- Margalit, B., Berger, E., & Metzger, B. D. 2019, ApJ, 886, 110, doi: [10.3847/1538-4357/ab4c31](https://doi.org/10.3847/1538-4357/ab4c31)
- Margalit, B., & Metzger, B. D. 2018, ApJL, 868, L4, doi: [10.3847/2041-8213/aaedad](https://doi.org/10.3847/2041-8213/aaedad)
- . 2019, ApJL, 880, L15, doi: [10.3847/2041-8213/ab2ae2](https://doi.org/10.3847/2041-8213/ab2ae2)
- McQuinn, M. 2014, ApJL, 780, L33, doi: [10.1088/2041-8205/780/2/L33](https://doi.org/10.1088/2041-8205/780/2/L33)
- Mereghetti, S., Savchenko, V., Ferrigno, C., et al. 2020, ApJL, 898, L29, doi: [10.3847/2041-8213/aba2cf](https://doi.org/10.3847/2041-8213/aba2cf)
- Metzger, B. D., Berger, E., & Margalit, B. 2017, ApJ, 841, 14, doi: [10.3847/1538-4357/aa633d](https://doi.org/10.3847/1538-4357/aa633d)
- Metzger, B. D., Margalit, B., & Sironi, L. 2019, MNRAS, 485, 4091, doi: [10.1093/mnras/stz700](https://doi.org/10.1093/mnras/stz700)
- Meurs, E. J. A., Vergani, S. D., O'Maoileidigh, C., Malesani, D., & Gualandi, R. 2006, GRB Coordinates Network, 5074, 1
- Michałowski, M. J. 2021, ApJL, 920, L21, doi: [10.3847/2041-8213/ac2b35](https://doi.org/10.3847/2041-8213/ac2b35)
- Muñoz, J. B., & Loeb, A. 2018, PhRvD, 98, 103518, doi: [10.1103/PhysRevD.98.103518](https://doi.org/10.1103/PhysRevD.98.103518)
- Murase, K., Kashiyama, K., & Mészáros, P. 2016, MNRAS, 461, 1498, doi: [10.1093/mnras/stw1328](https://doi.org/10.1093/mnras/stw1328)
- NASA/IPAC Extragalactic Database (NED). 2019, NASA/IPAC Extragalactic Database (NED), IPAC, doi: [10.26132/NED](https://doi.org/10.26132/NED)
- Navarro, J. F., Frenk, C. S., & White, S. D. M. 1997, ApJ, 490, 493, doi: [10.1086/304888](https://doi.org/10.1086/304888)
- Nicholl, M., Williams, P. K. G., Berger, E., et al. 2017, ApJ, 843, 84, doi: [10.3847/1538-4357/aa794d](https://doi.org/10.3847/1538-4357/aa794d)
- Nimmo, K., Hewitt, D. M., Hessels, J. W. T., et al. 2021, arXiv e-prints, arXiv:2111.01600. <https://arxiv.org/abs/2111.01600>
- Norris, J., Ukwatta, T. N., Barthelmy, S. D., et al. 2010a, GRB Coordinates Network, 11113, 1
- Norris, J. P., Barthelmy, S. D., Gehrels, N., & Grupe, D. 2010b, GRB Coordinates Network, 10427, 1
- Obenberger, K. S., Hartman, J. M., Taylor, G. B., et al. 2014, ApJ, 785, 27, doi: [10.1088/0004-637X/785/1/27](https://doi.org/10.1088/0004-637X/785/1/27)
- Palaniswamy, D., Wayth, R. B., Trott, C. M., et al. 2014, ApJ, 790, 63, doi: [10.1088/0004-637X/790/1/63](https://doi.org/10.1088/0004-637X/790/1/63)
- Pal'Shin, V., Golenetskii, S., Aptekar, R., et al. 2008, GRB Coordinates Network, 8256, 1
- Pan, Z., Yang, H., & Yagi, K. 2022, arXiv e-prints, arXiv:2208.08808. <https://arxiv.org/abs/2208.08808>
- Petroff, E., Hessels, J. W. T., & Lorimer, D. R. 2019, A&A Rv, 27, 4, doi: [10.1007/s00159-019-0116-6](https://doi.org/10.1007/s00159-019-0116-6)
- Petroff, E., & Yaron, O. 2020, Transient Name Server AstroNote, 160, 1
- Petroff, E., Bailes, M., Barr, E. D., et al. 2015, MNRAS, 447, 246, doi: [10.1093/mnras/stu2419](https://doi.org/10.1093/mnras/stu2419)
- Piro, L., Bruni, G., Troja, E., et al. 2021, A&A, 656, L15, doi: [10.1051/0004-6361/202141903](https://doi.org/10.1051/0004-6361/202141903)
- Planck Collaboration, Ade, P. A. R., Aghanim, N., et al. 2016, A&A, 594, A13, doi: [10.1051/0004-6361/201525830](https://doi.org/10.1051/0004-6361/201525830)
- Planck Collaboration, Aghanim, N., Akrami, Y., et al. 2020, A&A, 641, A6, doi: [10.1051/0004-6361/201833910](https://doi.org/10.1051/0004-6361/201833910)

- Platts, E., Weltman, A., Walters, A., et al. 2019, PhR, 821, 1, doi: [10.1016/j.physrep.2019.06.003](https://doi.org/10.1016/j.physrep.2019.06.003)
- Pleunis, Z., Good, D. C., Kaspi, V. M., et al. 2021, arXiv e-prints, arXiv:2106.04356.
<https://arxiv.org/abs/2106.04356>
- Poole, T. S., & Troja, E. 2006, GRB Coordinates Network, 5069, 1
- Pooley, D., Lewin, W. H. G., Anderson, S. F., et al. 2003, ApJL, 591, L131, doi: [10.1086/377074](https://doi.org/10.1086/377074)
- Popov, S. B., & Postnov, K. A. 2013, arXiv e-prints, arXiv:1307.4924. <https://arxiv.org/abs/1307.4924>
- Price, P. A., Berger, E., Fox, D. B., Cenko, S. B., & Rau, A. 2006, GRB Coordinates Network, 5077, 1
- Prieto, J. L., Stanek, K. Z., & Beacom, J. F. 2008, ApJ, 673, 999, doi: [10.1086/524654](https://doi.org/10.1086/524654)
- Prochaska, J. X., & Zheng, Y. 2019, MNRAS, 485, 648, doi: [10.1093/mnras/stz261](https://doi.org/10.1093/mnras/stz261)
- Prochaska, J. X., Macquart, J.-P., McQuinn, M., et al. 2019, Science, 366, 231, doi: [10.1126/science.aay0073](https://doi.org/10.1126/science.aay0073)
- Ravi, V., Catha, M., D'Addario, L., et al. 2019, Nature, 572, 352, doi: [10.1038/s41586-019-1389-7](https://doi.org/10.1038/s41586-019-1389-7)
- Rowlinson, A., Gourdji, K., van der Meulen, K., et al. 2019, MNRAS, 490, 3483, doi: [10.1093/mnras/stz2866](https://doi.org/10.1093/mnras/stz2866)
- Rowlinson, A., Starling, R. L. C., Gourdji, K., et al. 2021, MNRAS, 506, 5268, doi: [10.1093/mnras/stab2060](https://doi.org/10.1093/mnras/stab2060)
- Rumyantsev, V., Karimov, R., Salyamov, R., et al. 2006, GRB Coordinates Network, 5184, 1
- Safarzadeh, M., Prochaska, J. X., Heintz, K. E., & Fong, W.-f. 2020, ApJL, 905, L30, doi: [10.3847/2041-8213/abd03e](https://doi.org/10.3847/2041-8213/abd03e)
- Sakamoto, T., Barthelmy, S. D., Cummings, J. R., et al. 2016, GRB Coordinates Network, 19276, 1
- Sato, G., Barbier, L., Barthelmy, S., et al. 2006, GRB Coordinates Network, 5064, 1
- Shannon, R. M., Macquart, J. P., Bannister, K. W., et al. 2018, Nature, 562, 386, doi: [10.1038/s41586-018-0588-y](https://doi.org/10.1038/s41586-018-0588-y)
- Takahashi, I., Uehara, T., Yoshida, K., et al. 2006a, GRB Coordinates Network, 5073, 1
- . 2006b, GRB Coordinates Network, 5065, 1
- Tavani, M., Verrecchia, F., Casentini, C., et al. 2020, The Astronomer's Telegram, 13446, 1
- Tendulkar, S. P., Bassa, C. G., Cordes, J. M., et al. 2017, ApJL, 834, L7, doi: [10.3847/2041-8213/834/2/L7](https://doi.org/10.3847/2041-8213/834/2/L7)
- Tendulkar, S. P., Gil de Paz, A., Kirichenko, A. Y., et al. 2021, ApJL, 908, L12, doi: [10.3847/2041-8213/abdb38](https://doi.org/10.3847/2041-8213/abdb38)
- The CHIME/FRB Collaboration, :, Amiri, M., et al. 2021, arXiv e-prints, arXiv:2106.04352.
<https://arxiv.org/abs/2106.04352>
- The LIGO Scientific Collaboration, the Virgo Collaboration, the KAGRA Collaboration, et al. 2022, arXiv e-prints, arXiv:2203.12038.
<https://arxiv.org/abs/2203.12038>
- Thomas, J., Saglia, R. P., Bender, R., et al. 2009, ApJ, 691, 770, doi: [10.1088/0004-637X/691/1/770](https://doi.org/10.1088/0004-637X/691/1/770)
- Thornton, D., Stappers, B., Bailes, M., et al. 2013, Science, 341, 53, doi: [10.1126/science.1236789](https://doi.org/10.1126/science.1236789)
- Tian, J., Anderson, G. E., Hancock, P. J., et al. 2022, PASA, 39, e003, doi: [10.1017/pasa.2021.58](https://doi.org/10.1017/pasa.2021.58)
- Totani, T. 2013, PASJ, 65, L12, doi: [10.1093/pasj/65.5.L12](https://doi.org/10.1093/pasj/65.5.L12)
- Troja, E., Burrows, D. N., & Gehrels, N. 2006a, GRB Coordinates Network, 5093, 1
- Troja, E., King, A. R., O'Brien, P. T., Lyons, N., & Cusumano, G. 2008, MNRAS, 385, L10, doi: [10.1111/j.1745-3933.2007.00421.x](https://doi.org/10.1111/j.1745-3933.2007.00421.x)
- Troja, E., Barthelmy, S. D., Boyd, P. T., et al. 2006b, GRB Coordinates Network, 5055, 1
- Ukwatta, T. N., Baumgartner, W. H., Chester, M. M., et al. 2008, GRB Coordinates Network, 7203, 1
- Verbunt, F. 2003, in Astronomical Society of the Pacific Conference Series, Vol. 296, New Horizons in Globular Cluster Astronomy, ed. G. Piotto, G. Meylan, S. G. Djorgovski, & M. Riello, 245.
<https://arxiv.org/abs/astro-ph/0210057>
- Vink, J., & Kuiper, L. 2006, MNRAS, 370, L14, doi: [10.1111/j.1745-3933.2006.00178.x](https://doi.org/10.1111/j.1745-3933.2006.00178.x)
- Wadiasingh, Z., & Timokhin, A. 2019, ApJ, 879, 4, doi: [10.3847/1538-4357/ab2240](https://doi.org/10.3847/1538-4357/ab2240)
- Wang, F. Y., Wang, Y. Y., Yang, Y.-P., et al. 2020a, ApJ, 891, 72, doi: [10.3847/1538-4357/ab74d0](https://doi.org/10.3847/1538-4357/ab74d0)
- Wang, J.-S., Yang, Y.-P., Wu, X.-F., Dai, Z.-G., & Wang, F.-Y. 2016, ApJL, 822, L7, doi: [10.3847/2041-8205/822/1/L7](https://doi.org/10.3847/2041-8205/822/1/L7)
- Wang, W.-H., Xu, H., Wang, W.-Y., et al. 2021, MNRAS, 507, 2208, doi: [10.1093/mnras/stab2213](https://doi.org/10.1093/mnras/stab2213)
- Wang, X.-G., Li, L., Yang, Y.-P., et al. 2020b, ApJL, 894, L22, doi: [10.3847/2041-8213/ab8d1d](https://doi.org/10.3847/2041-8213/ab8d1d)
- Wang, X.-G., Zhang, B., Liang, E.-W., et al. 2018, ApJ, 859, 160, doi: [10.3847/1538-4357/aabc13](https://doi.org/10.3847/1538-4357/aabc13)
- Wang, Y.-F., & Nitz, A. H. 2022, arXiv e-prints, arXiv:2203.17222. <https://arxiv.org/abs/2203.17222>
- Xi, S.-Q., Tam, P.-H. T., Peng, F.-K., & Wang, X.-Y. 2017, ApJL, 842, L8, doi: [10.3847/2041-8213/aa74cf](https://doi.org/10.3847/2041-8213/aa74cf)
- Xin, L. P., Li, H. L., Wang, J., et al. 2021, ApJ, 922, 78, doi: [10.3847/1538-4357/ac1daf](https://doi.org/10.3847/1538-4357/ac1daf)
- Xu, H., Niu, J. R., Chen, P., et al. 2021, arXiv e-prints, arXiv:2111.11764. <https://arxiv.org/abs/2111.11764>
- Yamasaki, S., Totani, T., & Kawanaka, N. 2016, MNRAS, 460, 2875, doi: [10.1093/mnras/stw1206](https://doi.org/10.1093/mnras/stw1206)

- Yang, Y.-P., & Zhang, B. 2018, ApJ, 868, 31, doi: [10.3847/1538-4357/aae685](https://doi.org/10.3847/1538-4357/aae685)
- . 2021, ApJ, 919, 89, doi: [10.3847/1538-4357/ac14b5](https://doi.org/10.3847/1538-4357/ac14b5)
- Yao, J. M., Manchester, R. N., & Wang, N. 2017, ApJ, 835, 29, doi: [10.3847/1538-4357/835/1/29](https://doi.org/10.3847/1538-4357/835/1/29)
- Yi, S.-X., Du, M., & Liu, T. 2022, ApJ, 924, 69, doi: [10.3847/1538-4357/ac35e7](https://doi.org/10.3847/1538-4357/ac35e7)
- Zhai, M., Qiu, Y. L., Wei, J. Y., et al. 2006, GRB Coordinates Network, 5057, 1
- Zhang, B. 2014, ApJL, 780, L21, doi: [10.1088/2041-8205/780/2/L21](https://doi.org/10.1088/2041-8205/780/2/L21)
- . 2016, ApJL, 827, L31, doi: [10.3847/2041-8205/827/2/L31](https://doi.org/10.3847/2041-8205/827/2/L31)
- . 2017, ApJL, 836, L32, doi: [10.3847/2041-8213/aa5ded](https://doi.org/10.3847/2041-8213/aa5ded)
- . 2018a, ApJL, 867, L21, doi: [10.3847/2041-8213/aae8e3](https://doi.org/10.3847/2041-8213/aae8e3)
- . 2018b, The Physics of Gamma-Ray Bursts, doi: [10.1017/9781139226530](https://doi.org/10.1017/9781139226530)
- . 2020, ApJL, 890, L24, doi: [10.3847/2041-8213/ab7244](https://doi.org/10.3847/2041-8213/ab7244)
- . 2022, ApJ, 925, 53, doi: [10.3847/1538-4357/ac3979](https://doi.org/10.3847/1538-4357/ac3979)
- Zhang, B., Zhang, B.-B., Virgili, F. J., et al. 2009, ApJ, 703, 1696, doi: [10.1088/0004-637X/703/2/1696](https://doi.org/10.1088/0004-637X/703/2/1696)
- Zhang, B.-B., & Zhang, B. 2017, ApJL, 843, L13, doi: [10.3847/2041-8213/aa7633](https://doi.org/10.3847/2041-8213/aa7633)
- Zhang, G. Q., & Wang, F. Y. 2019, MNRAS, 487, 3672, doi: [10.1093/mnras/stz1566](https://doi.org/10.1093/mnras/stz1566)
- Zhang, G. Q., Yu, H., He, J. H., & Wang, F. Y. 2020, ApJ, 900, 170, doi: [10.3847/1538-4357/abaa4a](https://doi.org/10.3847/1538-4357/abaa4a)
- Zhang, R. C., & Zhang, B. 2022, ApJL, 924, L14, doi: [10.3847/2041-8213/ac46ad](https://doi.org/10.3847/2041-8213/ac46ad)
- Zhang, R. C., Zhang, B., Li, Y., & Lorimer, D. R. 2021, MNRAS, 501, 157, doi: [10.1093/mnras/staa3537](https://doi.org/10.1093/mnras/staa3537)

APPENDIX

A. SGRB SAMPLE

Table 1. SGRB sample.

Name	T ₉₀	RA	Dec	Err ^a	Redshift ^b	Ref	Name	T ₉₀	RA	DEC	Err ^a	redshift ^b	Ref
GRB150101B	0.018	188.02	-10.93	0.03	0.134	(12)(13)	GRB140402A	0.031	207.592	5.971	2.8	n/a	(12)(13)
GRB100628A	0.036	225.943	-31.653	2.1	n/a	(12)(13)	GRB090515	0.036	164.15	14.44	0.048	n/a	(12)(13)
GRB130822A	0.04	27.92	-3.21	0.043	n/a	(12)(13)	GRB210119A	0.05	282.8	-61.8	0.05	n/a	(12)(13)
GRB070923	0.05	184.623	-38.294	2.1	n/a	(12)(13)	GRB210119A	0.06	282.822	-61.767	1.5	n/a	(12)(13)
GRB170112A	0.06	15.232	-17.233	2.5	n/a	(12)(13)	GRB150101A	0.06	312.6	36.73	0.045	n/a	(12)(13)
GRB050925	0.07	303.49	34.329	1.4	n/a	(12)(13)	GRB090417A	0.072	34.993	-7.141	2.8	n/a	(12)(13)
GRB050509B	0.073	189.06	28.98	0.063	0.226	(12)(13)	GRB190326A	0.08	341.652	39.914	1.6	n/a	(12)(13)
GRB180718A	0.08	336.019	2.79	3.0	n/a	(12)(13)	GRB070810B	0.08	8.952	8.822	2.5	n/a	(12)(13)
GRB110420B	0.084	320.045	-41.277	2.2	n/a	(12)(13)	GRB070209	0.09	46.213	-47.376	2.8	n/a	(12)(13)
GRB051105A	0.093	265.279	34.916	2.6	n/a	(12)(13)	GRB170524A	0.1	319.49	48.61	0.072	n/a	(12)(13)
GRB161104A	0.1	77.89	-51.46	0.05	n/a	(12)(13)	GRB120305A	0.1	47.54	28.49	0.032	n/a	(12)(13)
GRB160601A	0.12	234.94	64.54	0.052	n/a	(12)(13)	GRB100206A	0.12	47.16	13.16	0.055	0.4068	(12)(13)
GRB140622A	0.13	317.17	-14.42	0.04	0.959	(12)(13)	GRB060502B	0.131	278.94	52.63	0.087	0.287	(12)(13)
GRB220412B	0.14	320.758	-0.261	1.6	n/a	(12)(13)	GRB090621B	0.14	313.47	69.03	0.068	n/a	(12)(13)
GRB150710A	0.15	194.47	14.32	0.047	n/a	(12)(13)	GRB210919A	0.16	80.25	1.31	0.067	n/a	(12)(13)
GRB201221D	0.16	171.06	42.14	0.072	1.046	(12)(13)	GRB130626A	0.16	273.128	-9.525	1.8	n/a	(12)(13)
GRB100702A	0.16	245.6969	-56.5316	0.04	n/a	(12)(13)	GRB180402A	0.18	251.93	-14.97	0.035	n/a	(12)(13)
GRB130603B	0.18	172.2	17.07	0.023	0.3564	(12)(13)	GRB151127A	0.19	19.48	-82.77	0.032	n/a	(12)(13)
GRB140516A	0.19	252.99	39.96	0.037	n/a	(12)(13)	GRB170428A	0.2	330.08	26.92	0.038	0.454	(12)(13)
GRB160624A	0.2	330.19	29.64	0.028	0.483	(12)(13)	GRB101224A	0.2	285.92	45.71	0.053	0.4536	(12)(13)
GRB081101	0.2	95.836	-0.112	1.7	n/a	(12)(13)	GRB061217	0.21	160.41	-21.12	0.1	0.827	(12)(13)
GRB200411A	0.22	47.66	-52.32	0.023	n/a	(12)(13)	GRB150423A	0.22	221.58	12.28	0.027	1.394	(12)(13)
GRB120229A	0.22	20.033	-35.796	1.9	n/a	(12)(13)	GRB050906	0.258	52.82	-14.61	4.0	n/a	(12)(13)
GRB181123B	0.26	184.37	14.6	0.025	1.754	(12)(13)	GRB130313A	0.26	236.41	-0.37	0.08	n/a	(12)(13)
GRB151228A	0.27	214.017	-17.665	1.8	n/a	(12)(13)	GRB050202	0.27	290.584	-38.73	2.3	n/a	(12)(13)
GRB130912A	0.28	47.59	14	0.025	n/a	(12)(13)	GRB191031D	0.29	283.29	47.64	0.028	n/a	(12)(13)
GRB160525B	0.29	149.38	51.21	0.025	n/a	(12)(13)	GRB130515A	0.29	283.44	-54.28	0.04	n/a	(12)(13)

Name	T ₉₀	RA	Dec	Err ^a	Redshift ^b	Ref	Name	T ₉₀	RA	DEC	Err ^a	redshift ^b	Ref
GRB190427A	0.3	280.217	40.304	2.4	n/a	(12)(13)	GRB170325A	0.3	127.483	20.526	2.0	n/a	(12)(13)
GRB141212A	0.3	39.12	18.15	0.043	0.596	(12)(13)	GRB140903A	0.3	238.01	27.6	0.023	0.351	(12)(13)
GRB100117A	0.3	11.27	-1.59	0.04	0.92	(12)(13)	GRB091109B	0.3	112.74	-54.09	0.04	n/a	(12)(13)
GRB090510	0.3	333.55	-26.58	0.01	0.903	(12)(13)	GRB071112B	0.3	260.213	-80.884	2.2	n/a	(12)(13)
GRB160408A	0.32	122.62	71.13	0.027	n/a	(12)(13)	GRB100625A	0.33	15.8	-39.09	0.03	0.452	(12)(13)
GRB140606A	0.34	201.799	37.599	2.4	0.384	(12)(13)	GRB160714A	0.35	234.49	63.809	2.7	n/a	(12)(13)
GRB101129A	0.35	155.921	-17.645	3.0	n/a	(12)(13)	GRB160411A	0.36	349.36	-40.24	0.037	n/a	(12)(13)
GRB210726A	0.39	193.29	19.19	0.035	n/a	(12)(13)	GRB111020A	0.4	287.05	-38.01	0.027	n/a	(12)(13)
GRB090305A	0.4	241.764	-31.572	2.3	n/a	(12)(13)	GRB081226A	0.4	120.527	-69.006	3.0	n/a	(12)(13)
GRB070724	0.4	27.81	-18.59	0.028	0.457	(12)(13)	GRB210605B	0.448	15.7456	-6.429	0.095	n/a	(13)
GRB140320A	0.45	281.86	-11.19	0.082	n/a	(12)(13)	GRB120521A	0.45	148.72	-49.42	0.03	n/a	(12)(13)
GRB050813	0.45	241.99	11.25	0.048	n/a	(12)(13)	GRB111117A	0.47	12.7042	23.0167	3.0	2.211	(12)(13)
GRB070429B	0.47	328.02	-38.83	0.01	0.904	(12)(13)	GRB160927A	0.48	256.24	17.33	0.028	n/a	(12)(13)
GRB160821B	0.48	279.98	62.39	0.037	0.16	(12)(13)	GRB150301A	0.48	244.3	-48.71	0.083	n/a	(12)(13)
GRB201006A	0.49	61.89	65.16	0.032	n/a	(12)(13)	GRB060801	0.49	213.01	16.98	0.025	1.131	(12)(13)
GRB110112A	0.5	329.93	26.46	0.028	n/a	(12)(13)	GRB080702	0.5	313.05	72.31	0.03	n/a	(12)(13)
GRB170127B	0.51	19.98	-30.36	0.033	n/a	(12)(13)	GRB120630A	0.6	353.29	42.55	0.008	n/a	(12)(13)
GRB101219A	0.6	74.59	-2.54	0.028	0.718	(12)(13)	GRB090815C	0.6	64.49	-65.943	2.7	n/a	(12)(13)
GRB080919	0.6	265.22	-42.37	0.027	n/a	(12)(13)	GRB200522A	0.62	5.68	-0.28	0.037	0.554	(12)(13)
GRB190610A	0.62	46.244	-7.66	1.9	n/a	(12)(13)	GRB180715A	0.68	235.085	-0.899	2.0	n/a	(12)(13)
GRB160726A	0.7	98.809	-6.617	1.3	n/a	(12)(13)	GRB140414A	0.7	195.31	56.902	4.0	n/a	(12)(13)
GRB080121	0.7	137.235	41.841	3.0	n/a	(12)(13)	GRB060313	0.74	66.62	-10.84	0.023	n/a	(12)(13)
GRB061201	0.76	332.13	-74.58	0.008	0.111	(12)(13)	GRB130716A	0.8	179.57	63.05	0.033	n/a	(12)(13)
GRB111126A	0.8	276.057	51.461	3.0	n/a	(12)(13)	GRB120804A	0.81	233.95	-28.78	0.023	n/a	(12)(13)
GRB200907B	0.83	89.03	6.91	0.028	n/a	(12)(13)	GRB150728A	0.83	292.23	33.92	0.067	n/a	(12)(13)
GRB140930B	0.84	6.35	24.29	0.027	n/a	(12)(13)	GRB070729	0.9	56.32	-39.32	0.042	n/a	(12)(13)
GRB200325B	0.96	167.55381	27.8196	0.082	n/a	(13)	GRB081211	0.97	328.12	-33.84	0.027	n/a	(12)(13)
GRB210704A	1	159.08	57.31	0.002	n/a	(13)	GRB121226A	1	168.64	-30.41	0.035	n/a	(12)(13)
GRB111222A	1	179.21983	69.07039	0.045	n/a	(13)	GRB080905	1	287.67	-18.88	0.027	0.1218	(12)(13)
GRB210413B	1.088	182.558	55.965	3.0	n/a	(12)(13)	GRB200219A	1.1	342.65	-59.1	0.05	n/a	(12)(13)
GRB180727A	1.1	346.67	-63.05	0.028	n/a	(12)(13)	GRB141205A	1.1	92.859	37.876	2.0	n/a	(12)(13)
GRB070707S	1.1	267.74396	-68.92422	0.008	n/a	(13)	GRB210323A	1.12	317.95	25.37	0.037	n/a	(12)(13)

Name	T ₉₀	RA	Dec	Err ^a	Redshift ^b	Ref	Name	T ₉₀	RA	DEC	Err ^a	redshift ^b	Ref
GRB150831A	1.15	221.02	-25.63	0.027	n/a	(12)(13)	GRB180204A	1.16	330.13	30.84	0.023	n/a	(12)(13)
GRB150120A	1.2	10.32	33.99	0.03	n/a	(12)(13)	GRB090426	1.2	189.08	32.99	0.008	2.609	(12)(13)
GRB070406	1.2	198.956	16.53	3.3	n/a	(12)(13)	GRB040924	1.2	31.5792	16.0167	0.06	0.859	(13)
GRB170728A	1.25	58.89	12.18	0.009	n/a	(12)(13)	GRB120403A	1.25	42.458	40.489	2.3	n/a	(12)(13)
GRB211023B	1.3	170.31	39.14	0.009	n/a	(12)(13)	GRB161004A	1.3	263.15	-0.95	0.009	n/a	(12)(13)
GRB070809	1.3	203.7833	-22.1333	3.0	0.2187	(12)(13)	GRB051210	1.3	330.17	-57.61	0.027	n/a	(12)(13)
GRB140129B	1.36	326.76	26.21	0.008	n/a	(12)(13)	GRB151205B	1.4	41.19	-43.461	2.3	n/a	(12)(13)
GRB100724A	1.4	194.54	-11.1	0.025	1.288	(12)(13)	GRB051221	1.4	328.7	16.89	0.023	0.5465	(12)(13)
GRB131004A	1.54	296.11	-2.96	0.009	0.717	(12)(13)	GRB190627A	1.6	244.83	-5.29	0.008	1.942	(12)(13)
GRB180805A	1.68	167.57	-45.33	0.033	n/a	(12)(13)	GRB220730A	1.7	225.014	59.495	0.11	n/a	(12)(13)
GRB080426	1.7	26.5	69.47	0.025	n/a	(12)(13)	GRB211106A	1.75	343.59	-53.23	0.057	n/a	(12)(13)
GRB151229A	1.78	329.37	-20.73	0.023	n/a	(12)(13)	GRB081024A	1.8	27.87	61.33	0.03	n/a	(12)(13)
GRB071227	1.8	58.13	-55.98	0.01	0.383	(12)(13)	GRB140611A	1.9	349.917	40.104	0.917	n/a	(12)(13)
GRB200826A	1.95	6.817	34.038	21.0	0.7481	(13)	GRB201008A	2	161.8588	46.1019	0.08	n/a	(13)
GRB170817A	2	197.45	-23.38	0.022	0.01	(13)	GRB070714	2	42.93	30.24	0.03	1.58	(12)(13)
GRB060121	2	137.46742	45.66039	0.005	n/a	(13)	GRB210618A	2.13	235.82	46.01	0.05	n/a	(8)(12)(13)
GRB090927	2.2	343.97	-70.98	0.011	1.37	(11)(12)(13)	GRB090607	2.3	191.17	44.11	0.062	n/a	(2)(12)(13)
GRB100213A	2.4	349.39	43.38	0.038	n/a	(12)(13)(18)	GRB100816A	2.9	351.74	26.58	0.008	0.8049	(12)(13)(17)
GRB050724	3	246.19	-27.54	0.003	0.258	(12)(13)(14)	GRB210217A	4.22	97.61	68.72	0.05	n/a	(9)(12)(13)
GRB080913A	8	65.73	-25.13	0.032	6.695	(12)(13)(19)	GRB160410A	8.2	150.69	3.48	0.008	1.717	(12)(13)(20)
GRB070714B	64	57.84	28.3	0.008	0.92	(1)(12)(13)	GRB061210	85.3	144.52	15.62	0.03	0.4095	(6)(12)(13)
GRB150424A	91	152.31	-26.63	0.008	0.3	(4)(12)(13)	GRB081211B	102	168.27	53.83	0.03	n/a	(10)(12)(13)
GRB171007A	105	135.6	42.82	0.032	n/a	(3)(12)(13)	GRB080123	115	338.95	-64.9	0.027	0.495	(12)(13)(21)
GRB111121A	119	154.76	-46.67	0.023	n/a	(7)(12)(13)	GRB061006	130	111.03	-79.2	0.008	0.4377	(12)(13)(15)
GRB080503	170	286.62	68.79	0.004	n/a	(12)(13)(16)	GRB050709	220	345.36	-38.98	0.008	0.1606	(5)(13)

Note.^a The localization uncertainty in units of arcmin.^b The n/a means that this SGRB does not have a redshift measurement.

The references: (1)(Barbier et al. 2007), (2)(Barthelmy et al. 2009), (3)(Barthelmy et al. 2017), (4)(Beardmore et al. 2015), (5)(Butler et al. 2005), (6)(Cannizzo et al. 2006), (7)(D'Elia et al. 2011), (8)(Fermi Gbm Team & Likely Short Grb 2021), (9)(Fletcher & Fermi GBM Team 2021), (10)(Golenetskii et al. 2008), (11)(Grupe et al. 2009), (12)https://swift.gsfc.nasa.gov/archive/grb_table.html/, (13)J-G source (<https://www.mpe.mpg.de/~jcg/grbgen.html#userconsent#>), (14)050724(Krimm et al. 2005), (15)(Krimm et al. 2006), (16)(Mao et al. 2008), (17)(Norris et al. 2010a), (18)(Norris et al. 2010b), (19)(Pal'Shin et al. 2008), (20)(Sakamoto et al. 2016) and (21)(Ukwatta et al. 2008).

B. FRB AND GRB 060502B HOST GALAXY PROPERTIES

Table 2. Host galaxy properties for FRBs and GRB 060502B.

Name	Instrument	Offset (kpc)	SFR ($M_{\odot} \text{ yr}^{-1}$)	$\log(M_*/M_{\odot})$	Repeater?	Ref
GRB060502B	Swift	73.0^{+19}_{-19}	$0.6^{+0.2}_{-0.2}$	11.85	—	(2)
FRB121102A	Arecibo	$0.8^{+0.1}_{-0.1}$	$0.15^{+0.04}_{-0.04}$	8.16	y	(1)(3)
FRB171020A	ASKAP	-	0.13	8.95	n	(1)
FRB180301A	Parkes	$10.2^{+3.0}_{-3.0}$	$1.93^{+0.58}_{-0.58}$	9.36	y	(1)(3)
FRB180916B	CHIME	$5.4^{+0.0}_{-0.0}$	$0.06^{+0.02}_{-0.02}$	9.33	y	(1)(3)
FRB180924B	ASKAP	$3.4^{+0.8}_{-0.8}$	$0.88^{+0.26}_{-0.26}$	10.12	n	(1)(3)(5)
FRB181030A	CHIME	0	$0.36^{+0.10}_{-0.10}$	9.76	y	(3)
FRB181112A	ASKAP	$3.1^{+15.7}_{-3.1}$	$0.37^{+0.11}_{-0.11}$	9.60	n	(3)(5)
FRB190102C	ASKAP	$2.3^{+4.2}_{-2.3}$	$0.86^{+0.26}_{-0.26}$	9.67	n	(1)(3)
FRB190523A	DSA-10	$27.2^{+22.6}_{-22.6}$	$0.09^{+0.03}_{-0.03}$	10.79	n	(1)(3)(5)
FRB190608B	ASKAP	$6.5^{+0.8}_{-0.8}$	$0.69^{+0.21}_{-0.21}$	10.06	n	(1)(3)
FRB190611B	ASKAP	$11.7^{+5.8}_{-5.8}$	$0.27^{+0.08}_{-0.08}$	8.88	n	(1)(3)
FRB190711A	ASKAP	$1.6^{+4.5}_{-4.5}$	$0.42^{+0.12}_{-0.12}$	8.91	y	(1)(3)
FRB190714A	ASKAP	$2.7^{+1.8}_{-1.8}$	$0.65^{+0.20}_{-0.20}$	10.15	n	(1)(3)
FRB191001A	ASKAP	$11.1^{+0.8}_{-0.8}$	$8.06^{+2.42}_{-2.42}$	10.67	n	(1)(3)
FRB191228A	ASKAP	$5.7^{+3.3}_{-3.3}$	$0.50^{+0.15}_{-0.15}$	9.73	n	(1)(3)
FRB200120E	CHIME	$20.1^{+3.0}_{-3.0}$	$0.89^{+0.27}_{-0.27}$	10.86	y	(1)(3)
FRB200430A	ASKAP	$1.7^{+2.2}_{-1.7}$	$0.26^{+0.08}_{-0.08}$	9.32	n	(1)(3)
FRB200906A	ASKAP	$5.9^{+2.0}_{-2.0}$	$0.48^{+0.14}_{-0.14}$	10.12	n	(1)(3)
FRB201124A	CHIME	$1.3^{+0.1}_{-0.1}$	$2.12^{+0.69}_{-0.28}$	10.20	y	(1)(3)
FRB220207C	DSA-110	7.4	$2.14^{+0.26}_{-0.26}$	9.90	n	(4)
FRB220307B	DSA-110	6.0	$3.52^{+1.18}_{-0.60}$	11.73	n	(4)
FRB220310F	DSA-110	13.3	$0.15^{+0.01}_{-0.01}$	10.75	n	(4)
FRB220319D	DSA-110	2.8	$1.17^{+0.75}_{-0.72}$	9.93	n	(4)
FRB220418A	DSA-110	10.6	$0.37^{+0.40}_{-0.27}$	10.83	n	(4)
FRB220506D	DSA-110	12.0	$7.01^{+0.43}_{-0.64}$	10.45	n	(4)
FRB220509G	DSA-110	6.9	$0.08^{+0.06}_{-0.04}$	11.13	n	(4)
FRB220825A	DSA-110	8.1	$1.34^{+0.04}_{-0.04}$	11.14	n	(4)
FRB220914A	DSA-110	2.8	$1.45^{+1.05}_{-0.61}$	9.99	n	(4)
FRB220920A	DSA-110	6.2	$0.39^{+0.02}_{-0.02}$	10.85	n	(4)

Name	Instrument	Offset (kpc)	SFR ($M_{\odot} \text{ yr}^{-1}$)	$\log(M_*/M_{\odot})$	Repeater?	Ref
FRB221012A	DSA-110	14.7	$0.49^{+0.44}_{-0.30}$	11.30	n	(4)

The references are as follows: (1) Bhandari et al. (2022), (2) Bloom et al. (2007), (3) <http://frbhosts.org>, (4) Law et al. (2023), and (5) Li & Zhang (2020).